



LUND UNIVERSITY

Behaviour and Analytical Design of Fire Exposed Steel Structures, Insulated with Gypsum Plaster Slabs

Pettersson, Ove

1978

[Link to publication](#)

Citation for published version (APA):

Pettersson, O. (1978). *Behaviour and Analytical Design of Fire Exposed Steel Structures, Insulated with Gypsum Plaster Slabs*. (Bulletin of Division of Structural Mechanics and Concrete Construction, Bulletin 64; Vol. Bulletin 64). Lund Institute of Technology.

Total number of authors:

1

General rights

Unless other specific re-use rights are stated the following general rights apply:

Copyright and moral rights for the publications made accessible in the public portal are retained by the authors and/or other copyright owners and it is a condition of accessing publications that users recognise and abide by the legal requirements associated with these rights.

- Users may download and print one copy of any publication from the public portal for the purpose of private study or research.
- You may not further distribute the material or use it for any profit-making activity or commercial gain
- You may freely distribute the URL identifying the publication in the public portal

Read more about Creative commons licenses: <https://creativecommons.org/licenses/>

Take down policy

If you believe that this document breaches copyright please contact us providing details, and we will remove access to the work immediately and investigate your claim.

LUND UNIVERSITY

PO Box 117
221 00 Lund
+46 46-222 00 00

OVE PETTERSSON

BEHAVIOUR AND ANALYTICAL DESIGN OF
FIRE EXPOSED STEEL STRUCTURES,
INSULATED WITH GYPSUM PLASTER SLABS

OVE PETTERSSON

BEHAVIOUR AND ANALYTICAL DESIGN OF
FIRE EXPOSED STEEL STRUCTURES,
INSULATED WITH GYPSUM PLASTER SLABS

Presented at the EUROGYPSUM Scientific and Technical
Committee Seminar in Turin, 21-22 September 1978

BEHAVIOUR AND ANALYTICAL DESIGN OF FIRE EXPOSED STEEL STRUCTURES, INSULATED WITH GYPSUM PLASTER SLABS

By Ove Pettersson, Prof., Dr., Civil Engineering Department, Lund
University, Lund, Sweden

A development of analytical design procedures, based on well-defined functional requirements, is an important task of the future fire research within different fields of the overall fire safety concept. Such procedures, successively replacing the present, internationally prevalent, schematic design methods, are necessary for getting an improved economy and for enabling more qualified and reliable fire safety analyses. A derivation of such analytical design systems is also in agreement with the present trend of development of the building codes and regulations in many countries towards an increased extent of functionally based requirements and performance criteria.

In the ideal case, a rational fire design methodology includes as essential components [1]

- * analytical modelling of relevant processes; verification of model validation and accuracy; determination of critical design parameters,
- * formulation of functional requirements, independent of choice of design process and expressed either in deterministic or probabilistic terms,
- * determination of design parameter values, and
- * verification by the means of a reliability analysis that the choice of safety factors leads to safety levels, which are consistent with the expressed functional requirements.

For a fire engineering design of load-bearing structures and partitions, a differentiated analytical procedure is permitted to be applied in Sweden, as one alternative, since about ten years. The procedure constitutes a direct design method based on temperature characteristics of the fully developed compartment fire as a function of the fire load density, the

ventilation of the fire compartment and the thermal properties of the structures enclosing the fire compartment. The design method is approved for a general practical use by the National Swedish Board of Physical Planning and Building [2]. For facilitating the practical application, design diagrams and tables are systematically produced, giving directly, on one hand, the design temperature state of the fire exposed structure, on the other, a transfer of this information to the corresponding design load-bearing capacity of the structure; c.f., for instance [3], [4], [5], [6].

1. Principles of an Analytical Design of Fire Exposed Structures

In a generalized summary way, an analytical design method for fire exposed structures, based on well-defined functional requirements, can be described according to Fig. 1.

The design fire load density, the fire compartment characteristics and the fire extinguishment and fire fighting characteristics constitute the basis for a determination of the design fire exposure, given as the gastemperature-time curve $T-t$ of the fully developed compartment fire. Depending on the type of practical application, the load-bearing function of the structure can be required to be fulfilled for

- * the complete fire process,
- * a shortened fire process, limited by the time t_{ext} , necessary for the fire to be extinguished under the most severe conditions, or
- * a shortened fire process, limited by the design evacuation time t_{esc} for the building.

Together with the structural design data, the design thermal properties and the design mechanical strength of the structural materials, the design fire exposure gives the design temperature state and the design load-carrying capacity R_d as the lowest value during the relevant fire process.

A direct comparison between the design load-carrying capacity R_d and the design load effect at fire S_d decides whether the structure can fulfil its required function or not at the fire exposure.

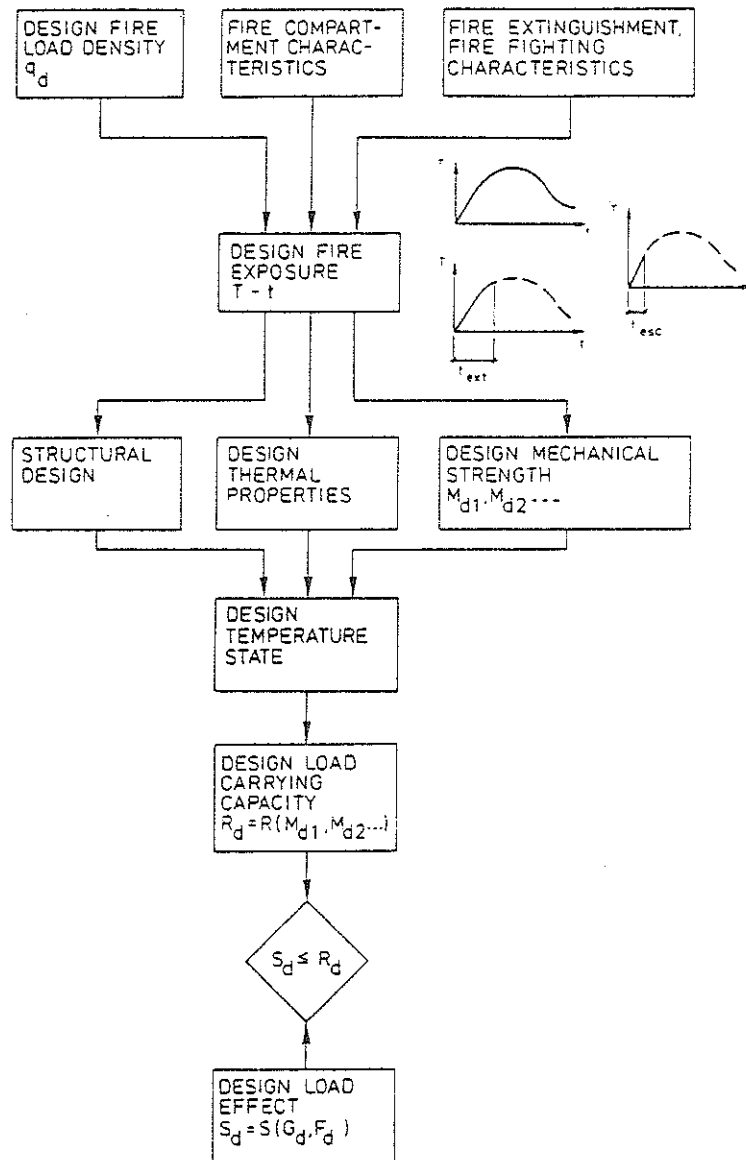


Figure 1. Procedure of an analytical design of fire exposed load-bearing structures

Following a recent draft of safety regulations [7], the determination of the design load effect S_d starts from characteristic values of permanent and variable loads G_k and F_k , connected to a defined probability of excess during a specified time period (Fig. 2). A multiplication by partial factors γ and load combination factors ψ transfers the characteristic load values to design loads G_d and F_d . The load combination factors ψ then may be differentiated with respect to whether a complete evacuation of people can be assumed or not in the event of fire. Finally, the design loads are combined and transformed to the design load effect at fire S_d .

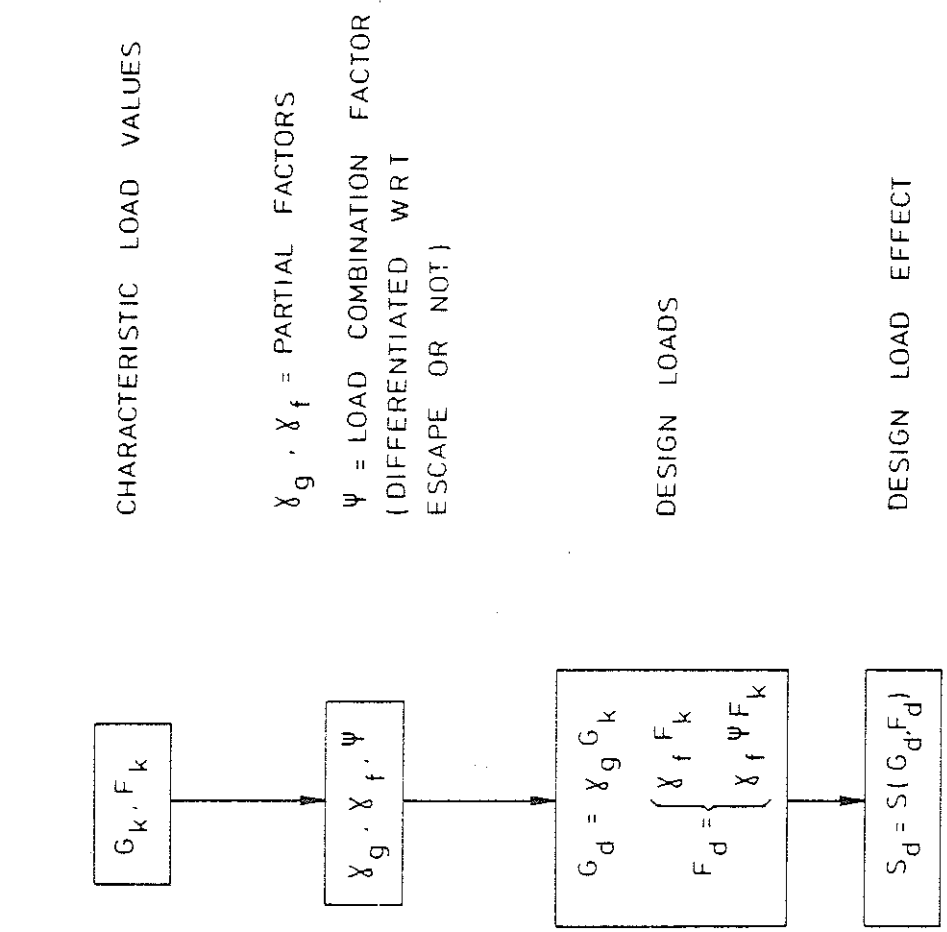


Figure 2. Procedure of determination of design load effect S_d

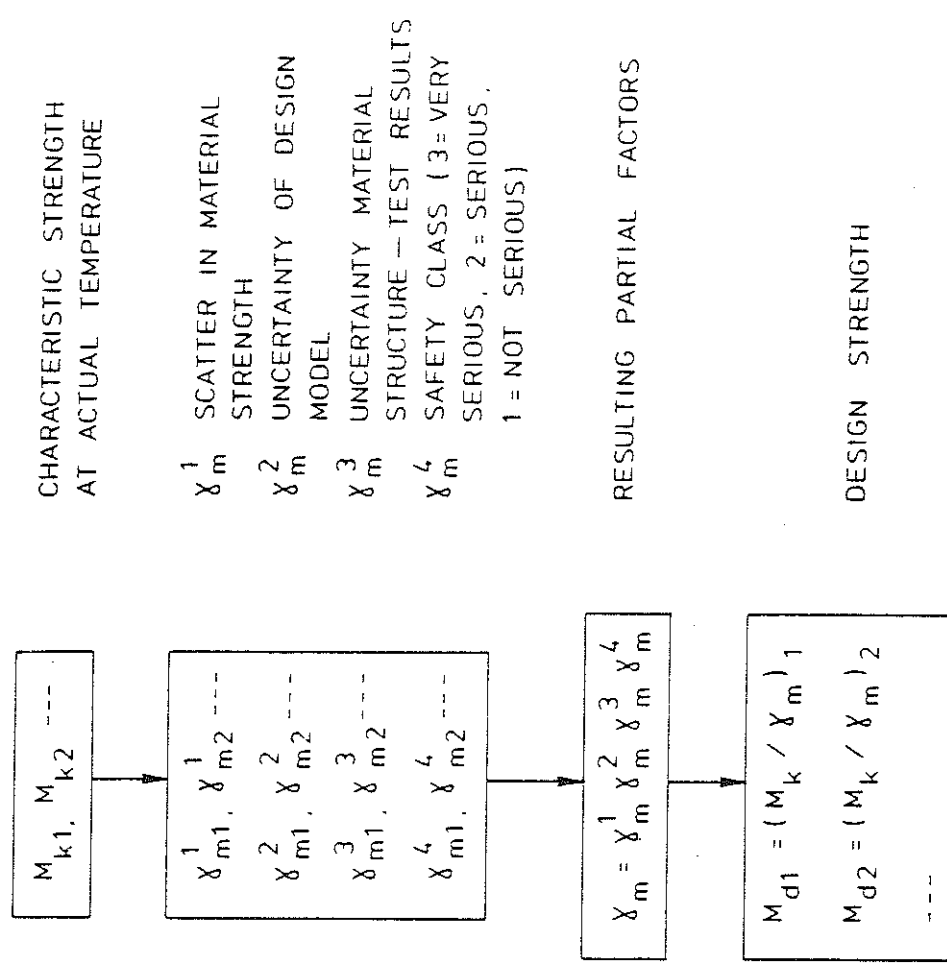


Figure 3. Procedure of determination of design strength M_d

Analogously, the design material strength M_d is to be calculated via characteristic strength values M_k at actual temperature, divided by resulting partial factors γ_m (Fig. 3). The characteristic strength values are defined as corresponding to specified fractiles of the probability density distribution. The different partial factors γ_m^1 , γ_m^2 , γ_m^3 , and γ_m^4 , are expressing the influence of the scatter in material strength, the uncertainty of the design model, the uncertainty in relation between material property in the structure and material property determined in test, and the safety class, respectively. The predicted extent of personal and property damage at failure - very serious, serious, not serious - decides the safety class.

A similar approach - as outlined for the design load effect S_d and the design mechanical strength M_d - can be applied also to the design fire load density q_d and the design thermal properties of the structural materials.

A methodology for a probabilistic analysis of fire exposed steel structures, connected to the described design method, has been developed in [8]. The methodology comprises a general systematized scheme for the identification and evaluation of the various sources and kinds of uncertainty in the differentiated structural fire engineering design. The structure of the methodology is quite general and applicable to a wide class of structures and structural elements.

Described in a more detailed way, a direct, differentiated, analytical design of fire exposed load-bearing structures or structural members, inside a fire compartment, includes the following steps - Fig. 4.

The basis of the design is given by the fully developed compartment fire exposure. Decisive entrance quantities then are

- (1) nominal load and load factor for fire load density,
- (2) combustion properties of this design fire load,
- (3) size and geometry of the fire compartment,
- (4) ventilation characteristics of the fire compartment, and
- (5) thermal properties of structures enclosing the fire compartment.

These quantities jointly determine the rate of burning, the rate of heat release, and the design gas temperature-time curve of the complete fire process. Together with

- (6) structural data for the proposed structure,
- (7) thermal properties of structural materials, and
- (8) coefficients of heat transfer for various surfaces of the structure

this design gas temperature-time curve gives the requisite information for a determination of the transient temperature fields of the fire exposed structure or structural members. With

- (9) mechanical properties of structural materials (Fig. 3), and
- (10) load characteristics

as further entrance quantities the time variation of restraint forces and moments, thermal stresses, and load-carrying capacity R can be determined. The lowest value of R during the complete fire process defines the design load-carrying capacity R_d .

Over nominal loads and load factors for dead load, live load, etc., statistically representative of a fire occasion, the design load effect at fire S_d is defined, interdependent on non-fire design procedure (Fig. 2).

A direct comparison between the design load-carrying capacity R_d and the design load effect at fire S_d decides whether the structure can fulfil its required function or not at a fire exposure.

For buildings containing activities, which are particularly important from, for instance, an economical point of view, there may be the motive for requiring that the building can be used again after a fire, almost immediately or very soon, for the current activities in a full extent. If a fire engineering design also includes such a requirement on re-serviceability of the structure after fire, the design procedure is to be as follows.

From the time curve of the load-carrying capacity R , the design residual load-carrying capacity R_{rd} of the structure after fire is obtained as an end information. This quantity R_{rd} must be compared with the design load effect at service, non-fire state, on the structure S_{rd} , given by the corresponding nominal loads and load factors for dead load, live load, etc.

For fire-exposed, exterior, load-bearing structures, the procedure for a direct, differentiated design will be modified. For such a structure,

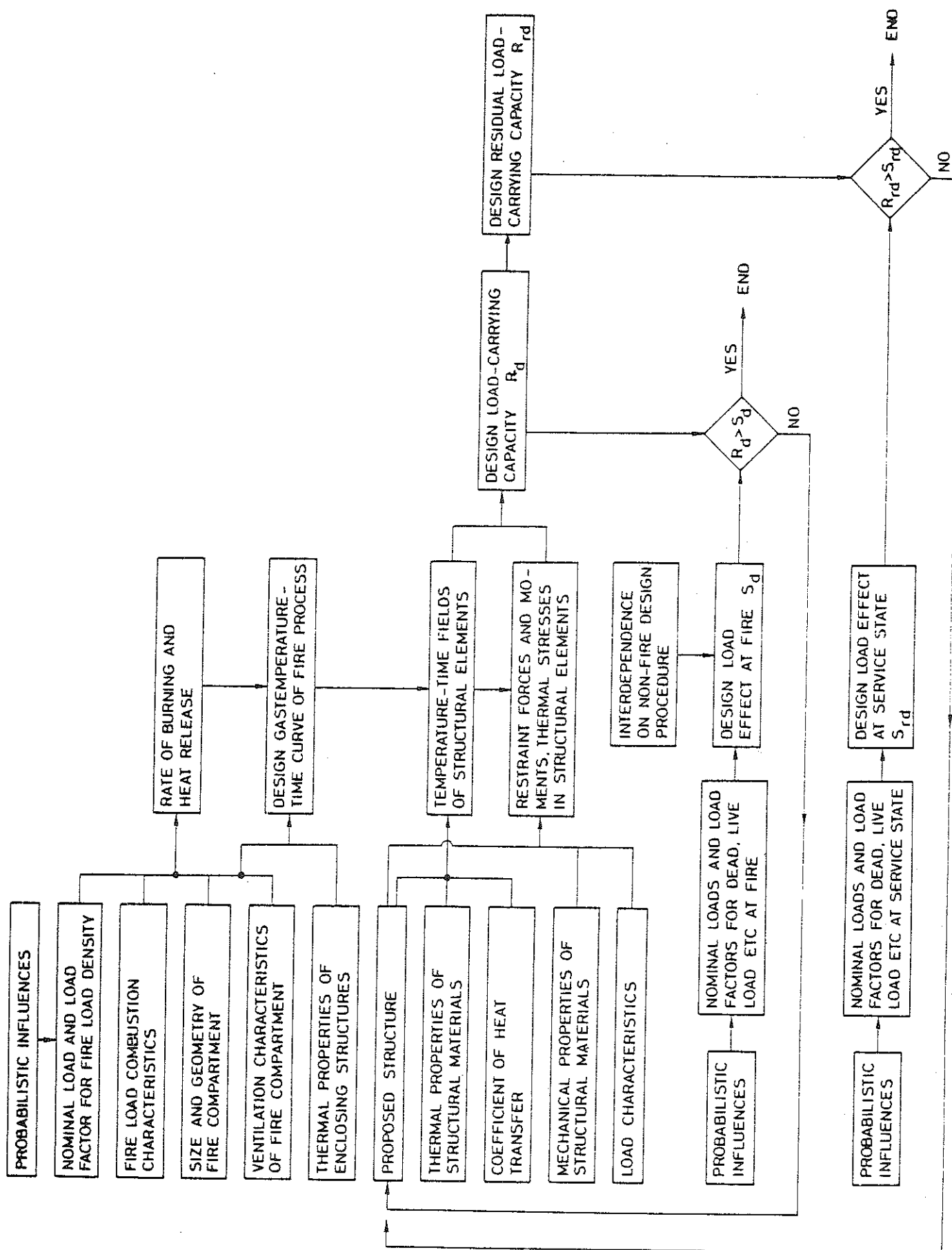


Figure 4. Procedure of a differentiated, analytical fire engineering design of load-bearing structures with additional requirement on re-serviceability after fire. Interior structures

the transient temperature fields are determined by a combined radiation and convection exposure from the flames and combustion gases outside the fire compartment as well as by radiation from the interior of the fire compartment through its window openings; cf., for instance [9], [10].

2. Fire Load Density and Gas Temperature-Time Curves of a Fully Developed Compartment Fire

At known combustion characteristics of the fire load, the gas temperature-time curve of a fully developed compartment fire can be calculated in the individual practical application from the heat and mass balance equations of the fire compartment with regard taken to the size, geometry and ventilation of the compartment, and to the thermal properties of the structures enclosing the compartment - Fig. 5 [2], [4], [6], [11], [12], [13], [14], [15], [16], [17].

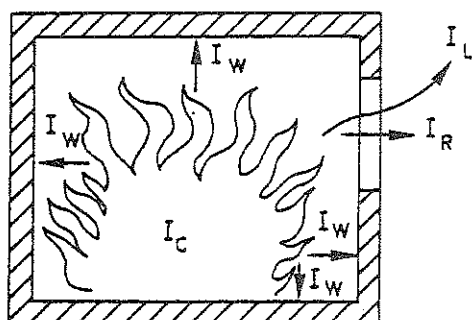


Figure 5. Energy balance equation $I_C = I_L + I_W + I_R$ of a fire compartment. I_C is the heat release per unit time from the combustion of the fuel, and I_L , I_W and I_R the quantities of energy removed per unit time by change of hot gases against cold air, by heat transfer to the surrounding structures, and by radiation through the openings of the compartment, respectively

For interior, load-bearing structures and partitions, the fire engineering design provisionally can be based on gas temperature-time curves T_t-t according to Fig. 6, [2], [4], [6], [13], which applies to a fire compartment with surrounding structures made of a material with a thermal conductivity $\lambda = 0.81 \text{ W} \cdot \text{m}^{-1} \cdot ^\circ\text{C}^{-1}$ and a heat capacity $\rho c_p = 1.67 \text{ MJ} \cdot \text{m}^{-3} \cdot ^\circ\text{C}^{-1}$ (fire compartment, type A). Entrance parameters of the diagrams are the fire load density q , defined by the formula

$$q = \frac{1}{A_t} \sum \mu_v m_v H_v \quad (\text{MJ} \cdot \text{m}^{-2}) \quad (1)$$

and the ventilation characteristics of the fire compartment, expressed by the opening factor $A\sqrt{h}/A_t$ ($m^{1/2}$), where

- A = total area of window and door openings (m^2),
- h = mean value of the heights of window and door openings, weighed with respect to each individual opening area (m),
- A_t = total interior area of the surfaces bounding the compartment, opening areas included (m^2),
- m_v = total weight of combustible material v (kg)
- H_v = effective heat value of combustible material v of the fire load ($MJ \cdot kg^{-1}$), and
- μ_v = a fraction between 0 and 1, giving the real degree of combustion for each individual component of the fire load.

The non-dimensional factor μ_v is a function of type of fuel, geometrical properties of fuel, and the position of fuel in a fire compartment, among other things. For some types of fire load components, μ_v will depend on the time of fire duration and on the gas temperature-time characteristics of the fire compartment. Bookcases and floor coverings are examples of fire components whose real degree of combustion is low, and whose μ_v values are probably appreciably below unity. At present, however, there is a lack of experimentally substantiated and verified μ_v values, and it is therefore usually necessary in the course of practical design to employ a fire load calculation with μ_v generally put equal to unity.

As a rule, the design fire load density is to be determined on the basis of statistical investigations for the type of building or premises in question. Such statistical investigations have been carried out for dwellings, offices, administration buildings, schools, stores, and hospitals [2], [4], [6]. As a temporary regulation, the Swedish Building Code authorizes the 80 percent level of the statistical distribution curve to be applied as the design fire load density.

The gas temperature-time curves in Fig. 6 have generally been determined on the assumption of ventilation controlled fires. For fires, which are fuel bed controlled in reality, this assumption leads to a structural fire engineering design on the safe side in practically every case, giving an overestimation of the maximum gastemperature and a simultaneous, partly

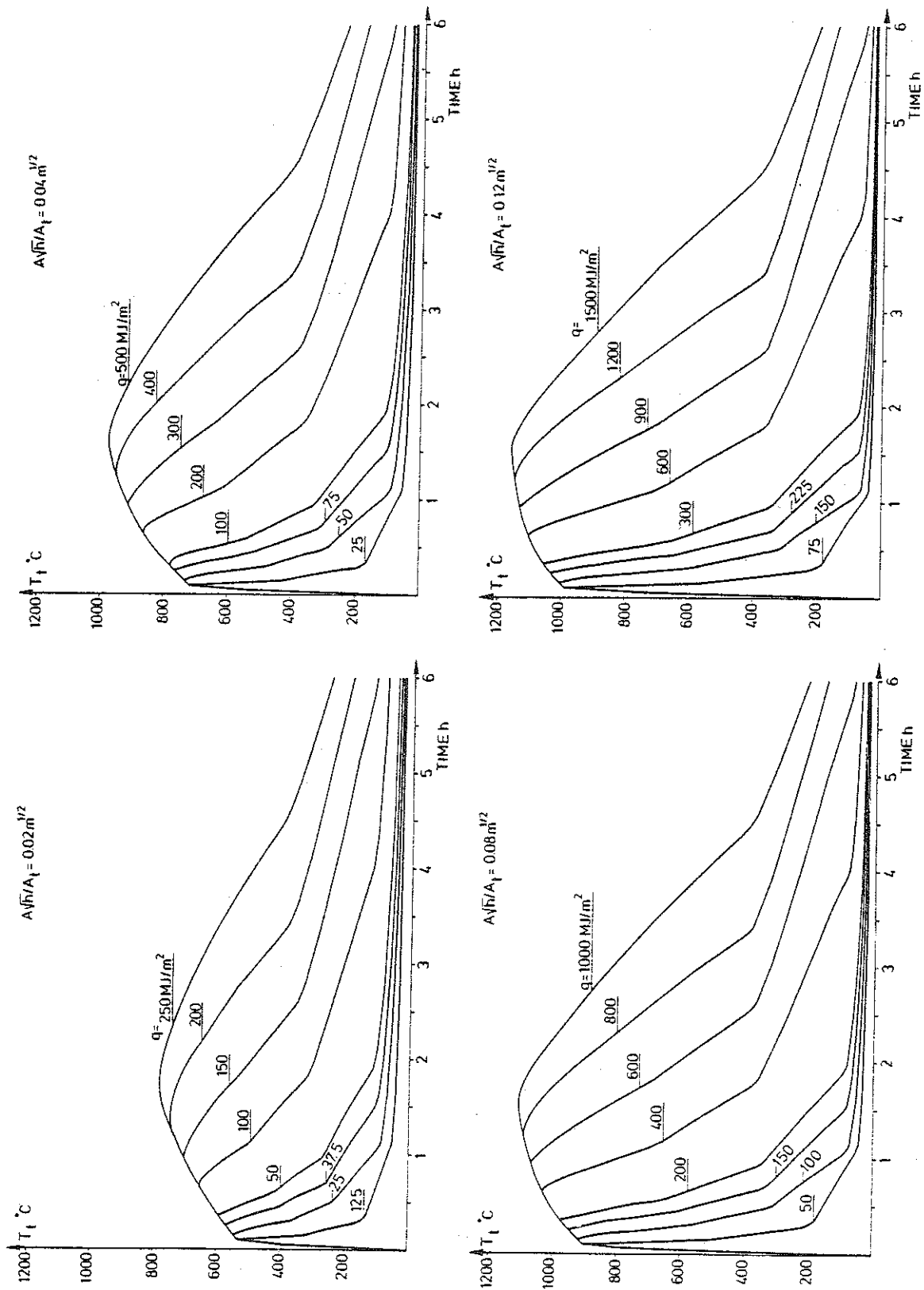


Figure 6. Gas temperature-time curves T_t - t of the complete process of fire development for different values of the fire load density q and the opening factor $A_f h / A_t$. Fire compartment, type A

balancing underestimation of the fire duration. For the minimum load-bearing capacity, which thermally can be seen as an integrated effect, the gas temperature-time curves in Fig. 6 give reasonably correct results, verified in [4], [8], [14].

As pointed out, the gas temperature-time curves in Fig. 6 apply to a certain fire compartment, type A, specified with respect to the thermal properties of its surrounding structures. Fire compartments with surrounding structures of deviating thermal properties can be transferred to fire compartment, type A, via fictitious values of the fire load density q_f and the opening factor $(A\sqrt{h}/A_t)_f$ in accordance to Table 1 in the appendix [2], [4], [6].

3. Design Temperature State of Fire Exposed Steel Structures and Partitions

For a fire exposed, uninsulated steel structure, the energy balance equation gives the following formula for a determination of the steel temperature-time curve T_s - t - Fig. 7

$$\Delta T_s = \frac{\alpha}{\rho_s c_{ps}} \cdot \frac{F_s}{V_s} (T_t - T_s) \Delta t \quad (^\circ\text{C}) \quad (2)$$

where

- ΔT_s = change of steel temperature ($^\circ\text{C}$) during time step Δt (s),
- α = coefficient of heat transfer at fire exposed surface of structure ($\text{W}\cdot\text{m}^{-2}\cdot^\circ\text{C}^{-1}$),
- ρ_s = density of steel material ($7850 \text{ kg}\cdot\text{m}^{-3}$),
- c_{ps} = specific heat of steel material ($\text{J}\cdot\text{kg}^{-1}\cdot^\circ\text{C}^{-1}$),
- F_s = fire exposed surface of steel structure per unit length (m),
- V_s = volume of steel structure per unit length (m^2),
- T_t = gas temperature ($^\circ\text{C}$) within fire compartment at time t (s).

Eq. (2) presupposes that the steel temperature T_s is uniformly distributed over the cross section of the structure at any time t .

The coefficient of heat transfer α can be calculated from the approximate formula

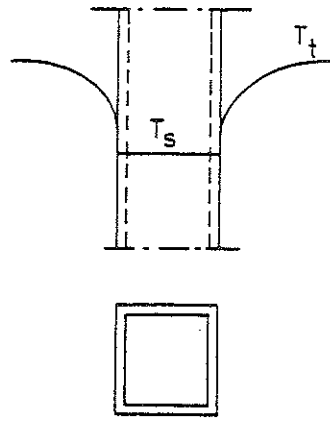


Figure 7. Fire exposed, uninsulated steel structure. T_t = gas temperature within fire compartment, T_s = steel temperature at time t

$$\alpha = 23 + \frac{5.77 \epsilon_r}{T_t - T_s} \left[\left(\frac{T_t + 273}{100} \right)^4 - \left(\frac{T_s + 273}{100} \right)^4 \right] \quad (\text{W} \cdot \text{m}^{-2} \cdot ^\circ\text{C}^{-1}) \quad (3)$$

giving an accuracy which is sufficient for ordinary practical purposes. ϵ_r is the resultant emissivity which for practical applications can be chosen according to the following table, giving values which generally are on the safe side.

1. Column, fire exposed on all sides	$\epsilon_r = 0.7$
2. Column, outside a facade	0.3
3. Floor structure, composed of steel beams with a concrete slab on the lower flange of the beams	0.5
4. Steel beams with a floor slab on the upper flange of the beams	
4a. Beams of I cross section with width/height ≥ 0.5	0.5
4b. Beams of I cross section with width/height < 0.5	0.7
4c. Beams of box cross section and trusses	0.7

In [2], [4], [5], [6], more accurate values are given for the resultant emissivity ϵ_r , as concerns the application case 4.

At a given gas temperature-time curve T_t - t of the fire compartment, the steel temperature T_s can be directly calculated from Eqs. (2) and (3) with regard taken to the temperature dependence of c_{ps} and α . Such computations have been carried out in a systematized way, giving the basis of design in Table 2 [4]. From this table, the maximum steel temperature $T_{s,\max}$ during a complete compartment fire can be determined directly as a function of the fictitious fire load density q_f , the fictitious opening

factor $(A\sqrt{h}/A_t)_f$, the F_s/V_s ratio and the resultant emissivity ϵ_r . The values of the table are connected to gas temperature characteristics according to Fig. 6.

For a fire exposed, insulated steel structure, analogously, a simplified energy balance equation gives the following formula for a direct determination of the steel temperature-time curve T_s-t - Fig. 8

$$\Delta T_s = \frac{A_i}{(1/\alpha + d_i/\lambda_i)\rho_s c_{ps} V_s} (T_t - T_s) \Delta t \quad (^\circ\text{C}) \quad (4)$$

with the additional quantities

A_i = interior jacket surface area of insulation per unit length (m),

d_i = thickness of insulation (m),

λ_i = thermal conductivity of insulating material ($\text{W}\cdot\text{m}^{-1}\cdot^\circ\text{C}^{-1}$).

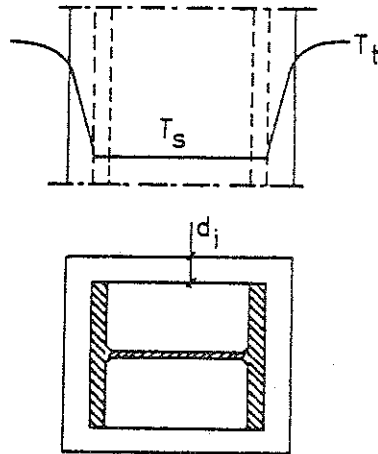


Figure 8. Fire exposed, insulated steel structure. T_t = gas temperature within fire compartment, T_s = steel temperature at time t

Eq. (4) presupposes that the steel temperature T_s is uniformly distributed over the cross section of the structure at any time t , that the temperature gradient is linear and the heating contribution negligible for the insulation, and that the heat transfer is one-dimensional.

Computations, originating from Eqs. (3) and (4), enable a production of a systematized design basis, facilitating an analytical, differentiated fire engineering design in practice. An example from such a design basis is referred in Table 3 [4], giving the maximum steel temperature $T_{s,\max}$ during a complete compartment fire for varying values of the fictitious fire load density q_f , the fictitious opening factor $(A\sqrt{h}/A_t)_f$, the structural parameter A_i/V_s , and the insulation parameter d_i/λ_i . The values of the table are connected to gas temperature characteristics according to Fig. 6.

Table 3 has been computed on the assumption of a constant thermal conductivity of the insulating material λ_i , chosen as an average value for the whole compartment fire process. Calculations, carried through systematically, are verifying that this average value of λ_i approximately coincides with the value, determined for an insulation temperature equal to the maximum steel temperature $T_{s,max}$.

For a specific insulating material, systematized design diagrams or tables can be computed very accurately with regard to the temperature dependence of the thermal properties of the steel as well as the insulating material. The influence of an initial moisture content and of a disintegration of the insulating material can be considered, too. Practically, such a determination can be carried out over a numerical data processing by computers on the basis of a finite difference or a finite element method. A great number of design tables, computed according to such an accurate procedure, are presented in [4]. Table 4 exemplifies this, giving the maximum steel temperature $T_{s,max}$ at varying fire and structural design characteristics for a fire exposed steel structure, insulated with gypsum plaster slabs, type Gyproc, of density $790 \text{ kg}\cdot\text{m}^{-3}$. The thermal properties of the gypsum plaster slabs then have been assumed to depend on the insulation temperature according to Fig. 9 [18], constructed on the basis of results from small scale and full scale tests and of information in the literature [19]. The influence of the disintegration of the slab material is considered.

In [4], an analytical model is derived for a simplified determination of the temperature-time fields of a steel beam construction according to Fig. 10 - composed of a reinforced concrete slab, load-bearing steel beams, and an insulating ceiling - exposed to a fire from below. By applying this computational model in a systematic way, a design basis has been determined, facilitating a calculation of the steel beam temperature T_s , assumed as uniformly distributed over the cross section of the beams. The design basis is exemplified in Table 5 [4], which gives the maximum steel beam temperature $T_{s,max}$ during a complete compartment fire for ^{varying} values of the fictitious fire load density q_f , the fictitious opening factor $(A\sqrt{h}/A_t)_f$, the structural parameter F_s/V_s , and the insulation parameter d_i/λ_i . F_s denotes the surface area of the steel beam, less the part covered by the concrete slab, and V_s the volume of the steel beam, per unit length. The

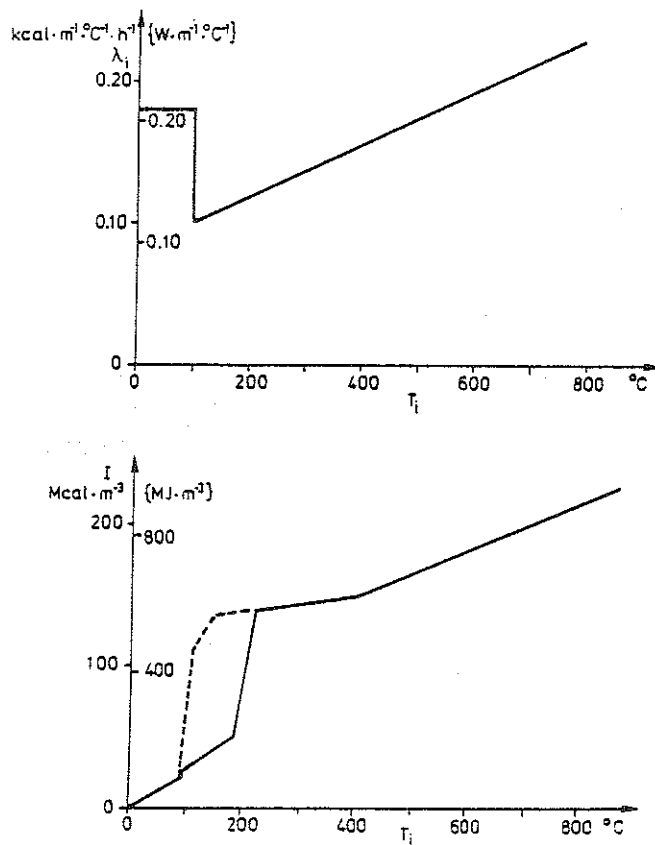


Figure 9. Thermal conductivity λ_i and enthalpy $I (= \int_0^T c_p dT)$ as a function of insulation temperature T_i for gypsum plaster slabs, type Gyproc, of density $790 \text{ kg}\cdot\text{m}^{-3}$. For enthalpy I , full line refers to a rapid heating and dashed line to a slow heating [18]

values, given in brackets in the table, denote the corresponding maximum temperature at the centre level of the ceiling. The values of the table are connected to gas temperature characteristics according to Fig. 6.

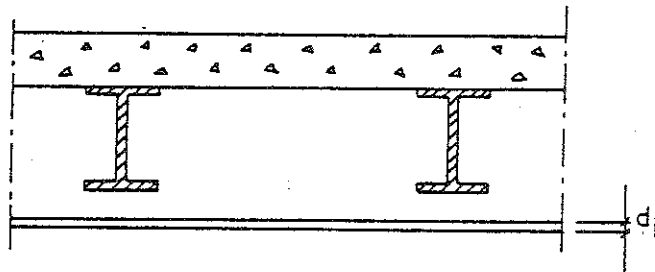


Figure 10. Floor structure, composed of a reinforced concrete slab, load-bearing steel beams, and an insulating ceiling

For several types of steel beam constructions with a suspended, insulating ceiling, the fire resistance of the ceiling and its fastening devices will be the decisive design criterion instead of the temperature of the steel beams. The ceiling can get a serious crack formation or fall down, partially or completely, after a comparatively short fire exposure. Under such conditions, the maximum steel beam temperature cannot be determined from Table 5 solely on the basis of the thickness d_i and the thermal conductivity λ_i of the ceiling. If results are available for a type of a suspended ceiling from a standard fire resistance test, these results can be used for deriving a fictitious value of the insulation parameter $d_i/\lambda_i - (d_i/\lambda_i)_{\text{fict}}$ - which describes the real fire behaviour of the suspended ceiling, including its fastening devices. From the test results, also a possible critical failure temperature of the suspended ceiling can be estimated. Cf., further [4].

After the determination of $(d_i/\lambda_i)_{\text{fict}}$ and the critical temperature of a type of a suspended ceiling, the analytical differentiated fire design can be carried out by a direct application of Table 5. Parallely, then the maximum temperature at the centre level of the ceiling according to the table must be controlled against the critical temperature of the ceiling.

Fictitious d_i/λ_i values and critical temperatures have been determined for a number of types of suspended ceilings in a series of standard fire resistance tests performed at the National Swedish Institute for Testing and Metrology in Stockholm [20]. The compositions of these suspended ceilings, the results obtained and the characteristics derived are set out in Table 6 [4].

The design basis, reproduced in Table 2 to 5, generally assumes the steel temperature to be uniformly distributed over the cross section of the beam or column at any time t . A more accurate theory, which enables a determination of the temperature variation over the cross section of the steel structure, is presented in [21], together with computer routines. The algorithm described can easily be coupled to most finite element programs. An illustration of the capability of the theory is given in Fig. 11, which shows calculated temperature distribution along the line of symmetry of a gypsum insulated steel beam with a concrete slab at the top flange at selected times of a standard fire resistance test according to ISO 834.

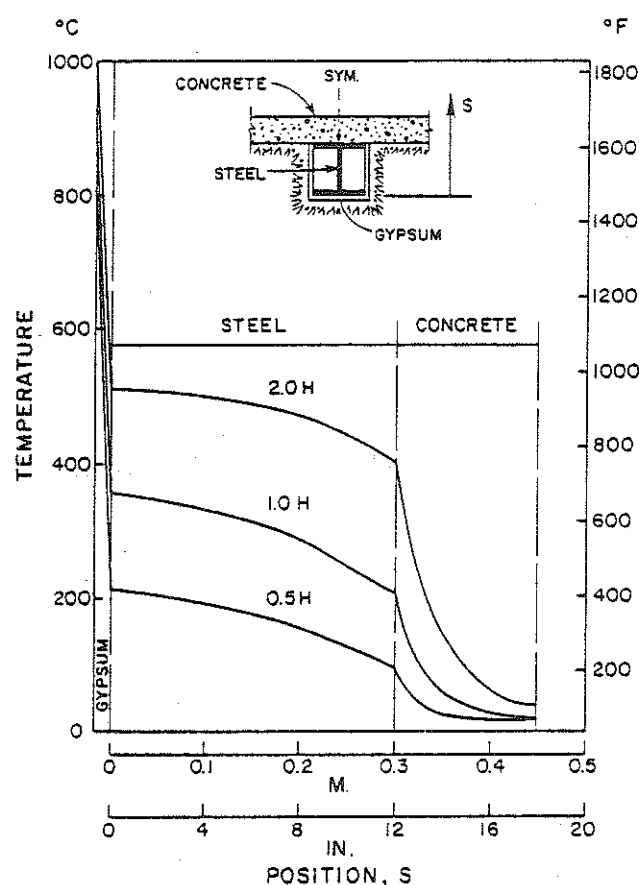


Figure 11. Calculated temperature distribution along line of symmetry of a steel beam, insulated by a 16 mm gypsum board (density $770 \text{ kg}\cdot\text{m}^{-3}$) and carrying a 150 mm concrete slab on top flange, at selected times of a thermal exposure according to ISO 834 [21]

As a complement to the design temperature state of fire exposed load-bearing steel structures, dealt with above, also some remarks will be given on the fire engineering design of partitions. The performance requirements for partitions imply that these must prevent a penetration of flames and hot gases and limit the rise in temperature on the unexposed side of the construction during a complete compartment fire.

An analytical method for a determination of the temperature-time field in a multi-layer partition is presented in [18]; cf. also [4]. The method considers the temperature dependence of the thermal material properties, an initial moisture content, and a possible material disintegration at specified temperature criteria. An illustrating application of the method is shown in Fig. 12 [18], which gives a summary conception

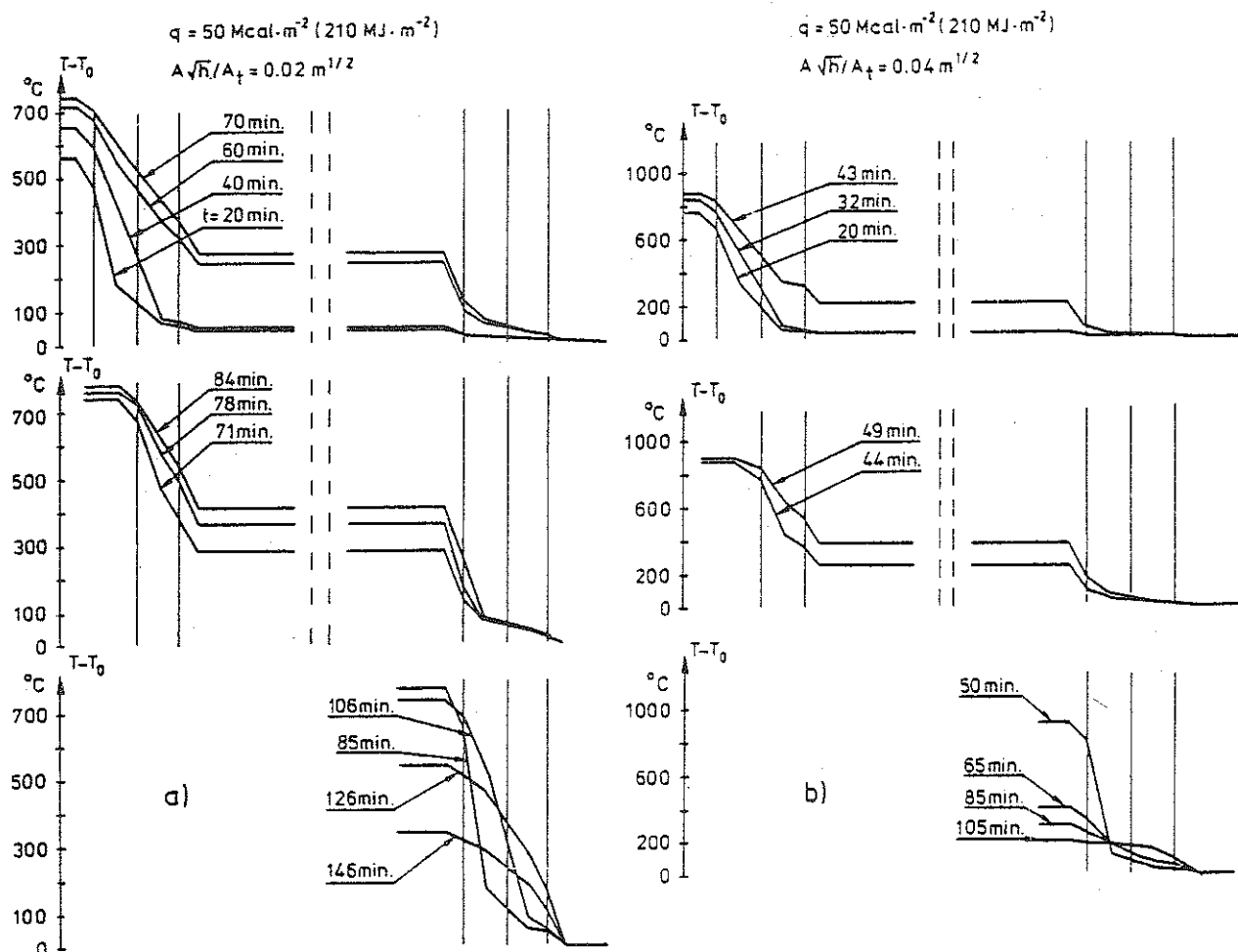


Figure 12. Calculated temperature-time fields for a steel stud wall, insulated on each side with two 13 mm gypsum plaster sheets, type Gyproc, of density $790 \text{ kg}\cdot\text{m}^{-3}$. The wall is fire exposed on one side with compartment fire characteristics according to Fig. 6: a) $q = 50 \text{ Mcal}\cdot\text{m}^{-2}$ ($210 \text{ MJ}\cdot\text{m}^{-2}$), $A\sqrt{h}/A_t = 0.02 \text{ m}^{1/2}$; b) $q = 50 \text{ Mcal}\cdot\text{m}^{-2}$ ($210 \text{ MJ}\cdot\text{m}^{-2}$), $A\sqrt{h}/A_t = 0.04 \text{ m}^{1/2}$. T_0 = temperature at time $t = 0$ [18]

of the fire behaviour of a steel stud wall, insulated on each side with two 13 mm gypsum plaster sheets, type Gyproc, of density $790 \text{ kg}\cdot\text{m}^{-3}$, fire exposed on one side and acting as a partition. The behaviour has been determined on the basis of temperature dependent thermal properties of gypsum plaster material according to Fig. 9 and a critical failure temperature for a gypsum plaster sheet of 550°C on that side of the sheet facing away from the fire. The results of full scale fire tests confirm this failure criterion.

Fig. 12a describes the fire behaviour of the wall, when it is fire exposed on one side by a compartment fire with gas temperature-time

characteristics according to Fig. 6 - fire load density $q = 50 \text{ Mcal} \cdot \text{m}^{-2}$ ($210 \text{ MJ} \cdot \text{m}^{-2}$), opening factor $A\sqrt{h}/A_t = 0.02 \text{ m}^{1/2}$. The figure gives a calculated failure of the directly fire exposed gypsum plaster sheet after about 70 min and of the next gypsum plaster sheet after about 85 min. The maximum temperature rise on the unexposed side of the wall amounts to 180°C during the complete fire process, i.e. precisely the maximum permissible value according to [2]. Fig. 12b analogously describes the fire behaviour of the wall, when it is exposed to a more rapid compartment fire - opening factor $A\sqrt{h}/A_t = 0.04 \text{ m}^{1/2}$ - at the same fire load density q . The increase of the opening factor results in a considerably decreased value of the maximum temperature rise on the unexposed side of the wall, which amounts to only about 55°C in this case.

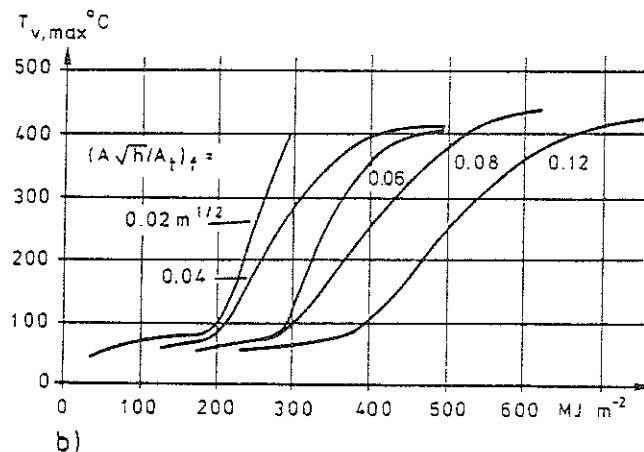
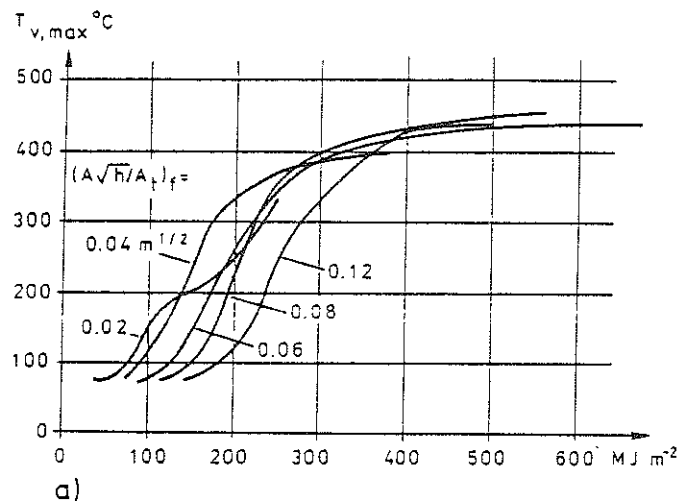


Figure 13. Maximum temperature $T_{v,max}$ during a complete fire process according to Fig. 6 on the unexposed side of a steel-gypsum plaster sheeting wall as a function of the fictitious fire load density q_f and the fictitious opening factor $(A\sqrt{h}/A_t)_f$ of the fire compartment. The wall is insulated on each side with one (fig a) or two (fig b) 13 mm gypsum plaster sheets, type Gyproc, of density $790 \text{ kg} \cdot \text{m}^{-3}$ [4], [6]

Systematic calculations of the type, illustrated by Fig. 12, lead to design diagrams as shown in Fig. 13 [4], [6], giving the maximum temperature $T_{v,max}$ during a complete fire process on the unexposed side of a steel stud-gypsum plaster sheeting wall as a function of the fictitious fire load density q_f and the fictitious opening factor of the fire compartment $(A\sqrt{h}/A_t)_f$. The two diagrams apply to an insulation on each side of the wall with one and two 13 mm gypsum plaster sheets, type Gyproc, of density $790 \text{ kg}\cdot\text{m}^{-3}$, respectively. The calculated $T_{v,max}$ values are to be compared with the corresponding maximum temperature, permitted in the Swedish Building Code, which implies 200°C as an average temperature and 240°C as a temperature over limited areas of the unexposed side of the partition [2].

4. Design Load-Bearing Capacity of Fire Exposed Steel Structures

By applying the design tables 2 to 5, the maximum steel temperature $T_{s,max}$ can be determined comparatively quickly for an uninsulated or insulated steel structure, exposed to a complete compartment fire with gas temperature-time characteristics according to Fig. 6. The corresponding design load-bearing capacity of the structure then is obtained by design diagrams of the type exemplified in Fig. 14, 15 and 16.

Fig. 14 and 15 [4], [6] give the design load-bearing capacity (M_{cr} , P_{cr} , q_{cr}) of fire exposed beams of constant I cross section at different types of loading and support conditions, as a function of the steel beam temperature T_s . The design curves in Fig. 14 apply to a slow rate of heating - assumed to be $4^\circ\text{C}\cdot\text{min}^{-1}$, followed by a cooling with a rate of $1.33^\circ\text{C}\cdot\text{min}^{-1}$ - and Fig. 15 gives the correction $\Delta\beta$ of the load-bearing capacity coefficient β due to a more rapid rate of heating. In the formulas for the load-bearing capacity

σ_s = yield stress of steel material at room temperature (MPa),

L = span of beam (m),

W = elastic modulus of beam cross section (m^3).

The design curves in Fig. 14 and 15 have been determined on the basis of the deformation curve of the fire exposed beams calculated by an

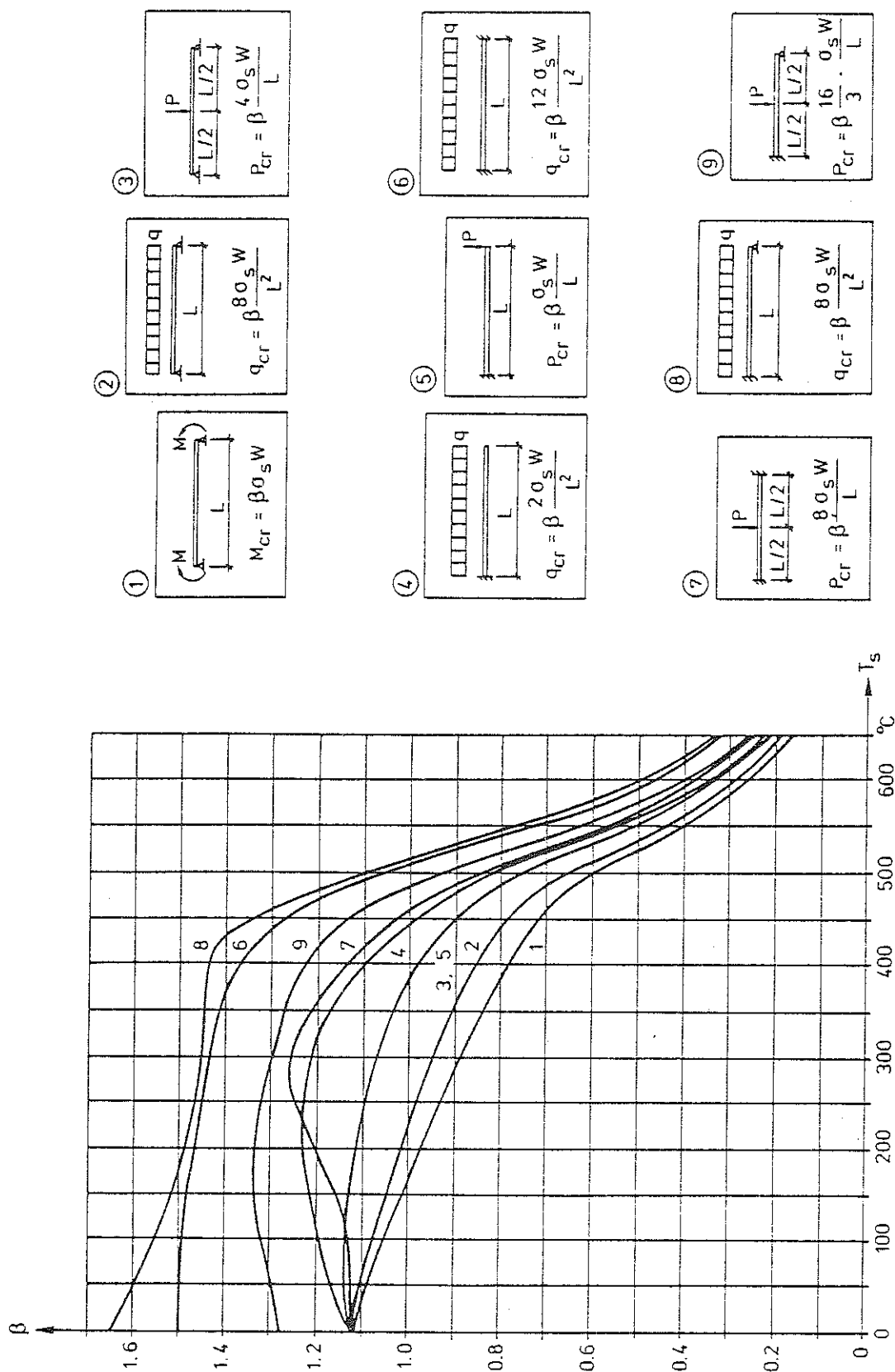


Figure 14. Coefficient β for determination of critical load (M_{cr} , P_{cr} , q_{cr}) for fire exposed beams of I cross section at different types of loading and support conditions, as a function of the steel beam temperature T_s . The curves have been calculated for a slow rate of heating of $4^{\circ}\text{C}\cdot\text{min}^{-1}$ and a subsequent cooling, assumed to be one third of the rate of heating [4], [6]

analytical model, presented in [22], which takes into account the softly rounded shape of the stress-strain curve of steel at elevated temperatures as well as the influence of creep strain. As can be seen from Fig. 15, this influence of creep begins to be noticeable for ordinary structural steels at temperatures in excess of about 450°C . The load-bearing capacity of the beams is defined by the limit deflection criterion according to ROBERTSON and RYAN [23].

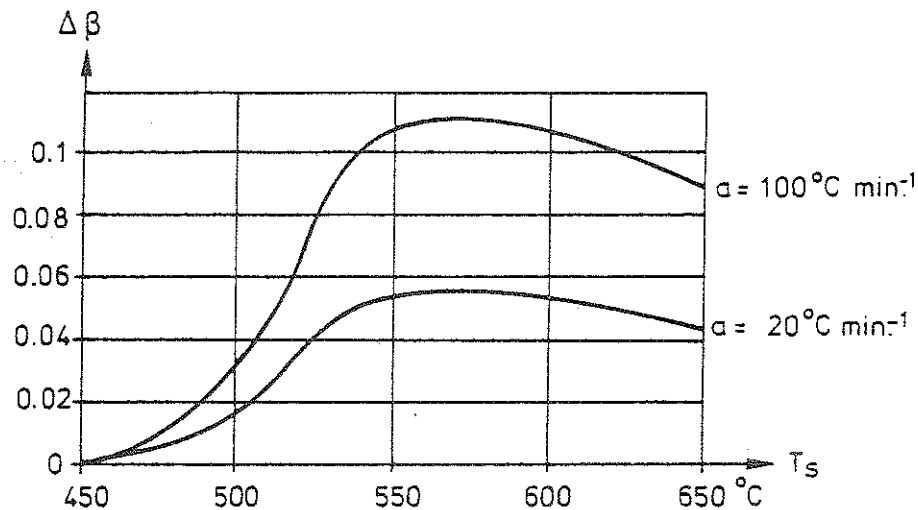


Figure 15. Increase $\Delta\beta$ of coefficient β , determined according to Fig. 14, for a rate of heating $\alpha \geq 4^{\circ}\text{C}\cdot\text{min}^{-1}$, as a function of the steel beam temperature T_s [4], [6]

The diagrams in Fig. 16 [4] determine the variation with the steel temperature T_s of the relationship between the buckling stress σ_{cr} and the slenderness ratio λ for fire exposed columns, axially loaded in compression. The diagrams apply to steel having a yield stress at room temperature $\sigma_s = 220, 260$ and 320 MPa, respectively, and are valid under the presumption that the column is unrestrained with respect to longitudinal expansion during the fire exposure. The σ_{cr} - λ curves have been computed for an initially deflected and excentrically loaded column on the basis of data on the change of the 0.5 % proof stress $\sigma_{0.5}$ and the secant modulus with the temperature, obtained in tension tests at a very slow rate of loading. This implies that a considerable influence of short-time creep at elevated temperatures is included.

For a fire engineering design of columns, partly restrained to a longitudinal expansion, reference is made to [4].

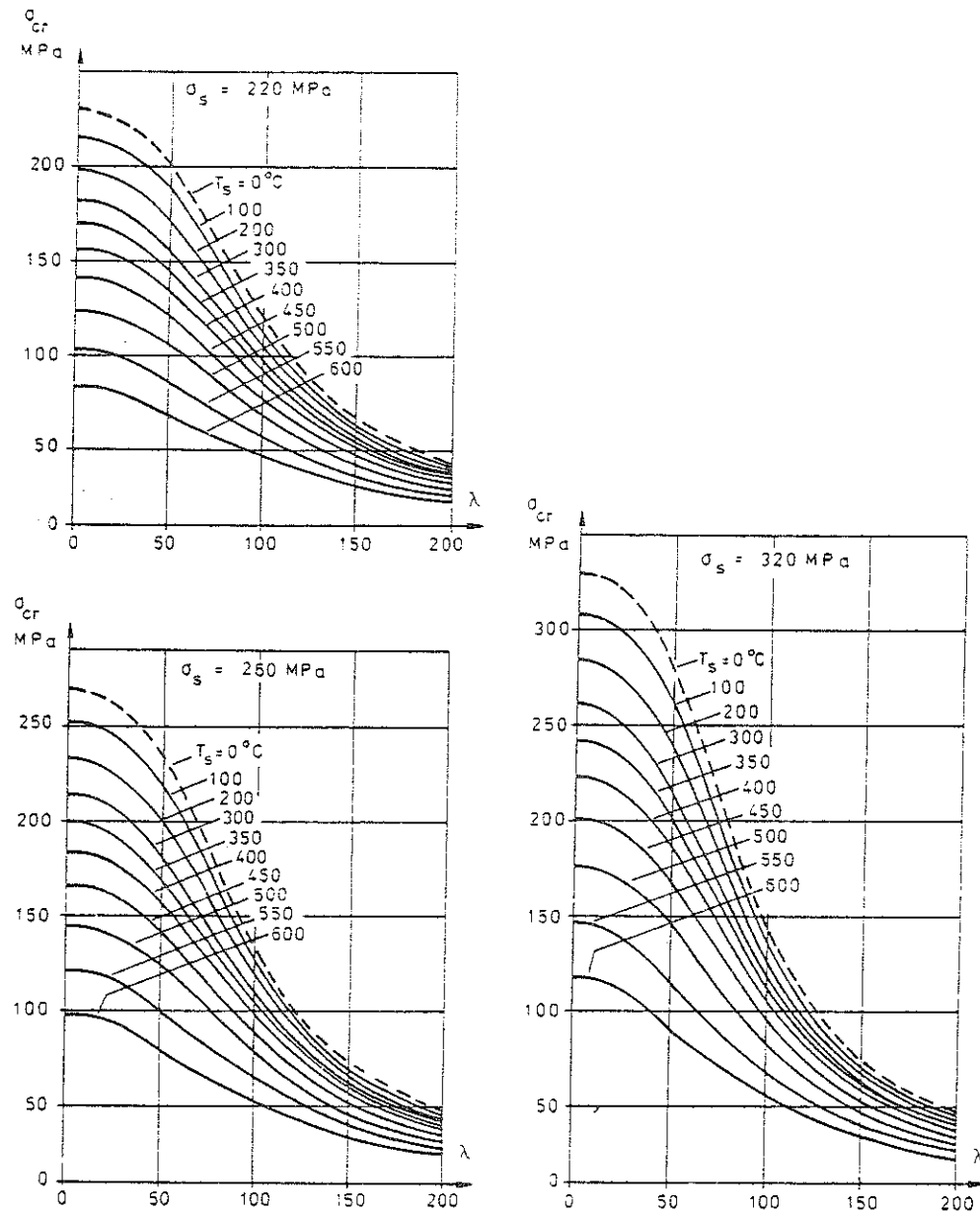


Figure 16. Variation with steel temperature T_s of the relationship between buckling stress σ_{cr} and slenderness ratio λ for fire exposed steel columns, axially loaded in compression, free to expand longitudinally and made of steel having a yield stress at room temperature $\sigma_s = 220$, 260 and 320 MPa, respectively [4], [6]

The design curves, reproduced in Fig. 14, 15 and 16, are generally based on the assumption of a uniformly distributed temperature over the cross section of the steel structure at any time t during the fire exposure. By this assumption, the design curves are directly connected to Tables 2 to 5, determining the design temperature state of the steel structure.

If the analytical, differentiated design of fire exposed steel structures will be further developed in future towards a more accurate determination

of the design temperature state, with regard taken to the temperature variation over the cross section of the steel structure, this will also require a more refined basis of design for the transfer of the design temperature state to the design load-bearing capacity of the fire exposed structure. The first attempts of developing such a more refined design basis now can be noticed in the literature. As a fragmentary example of this development, Fig. 17 [24] shows the calculated variation of the plastic bending moment of a fire exposed steel I cross section as a function of the maximum temperature for various linear temperature distributions over the cross section.

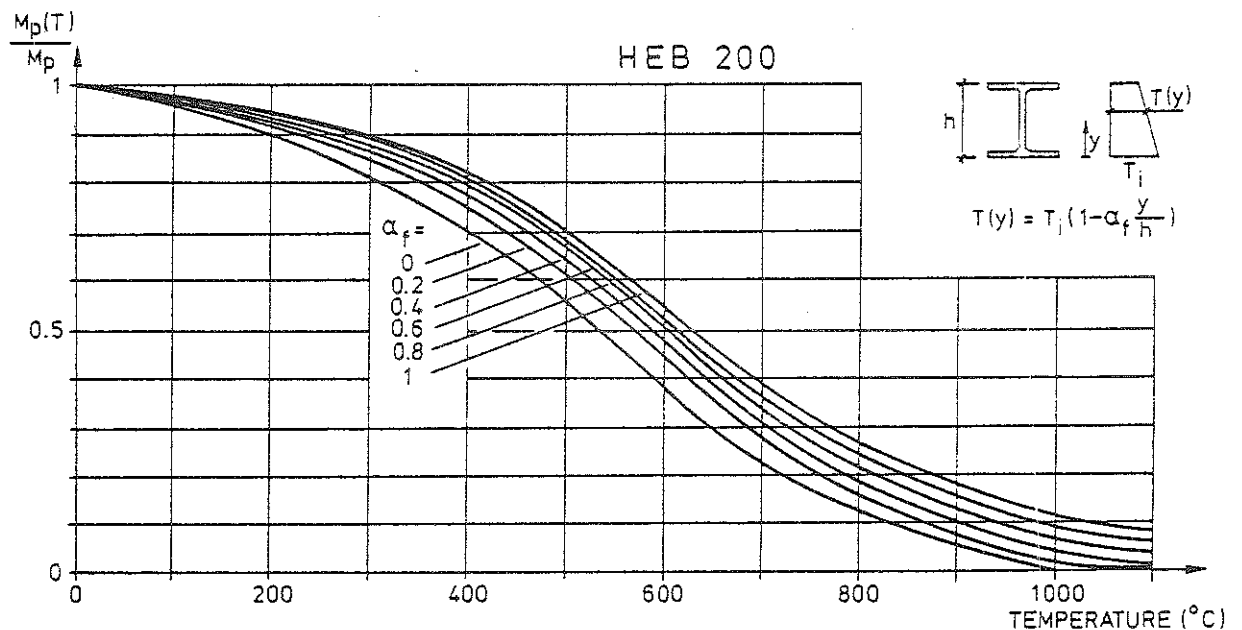


Figure 17. Calculated variation of plastic bending moment $M_p(T)$ in terms of various linear temperature distribution over height of a steel I cross section [24]

5. Summary

A differentiated procedure is presented for an analytical fire engineering design of load-bearing steel structures and partitions. The procedure is a direct design method based on gas temperature-time characteristics of a complete compartment fire, which depend on the fire load density, the ventilation of the fire compartment and the thermal properties of the structures enclosing the fire compartment. The practical use of the design procedure has been approved by the National Swedish Board of Physical Planning and Building.

For the practical application of the design procedure, a comprehensive design basis in the form of diagrams and tables has been worked out for a direct determination of the maximum steel temperature during a complete compartment fire and the corresponding design load-bearing capacity of the fire exposed structure. This design basis is exemplified in the paper, focused to steel structures with an insulation of gypsum plaster slabs, primarily for giving a rough impression of the character of the analytical design procedure.

Compared with the conventional fire engineering design, based on classification and results of standard fire resistance tests, the presented analytical design procedure has a more logical structure, based on well-defined functional requirements and performance criteria, gives a structural fire design with a better economy, and leads to a more consistent fire safety level.

References

- [1] MAGNUSSON, S.E. and PETTERSSON, O.: Functional Approaches - An Outline. Final Report, CIB W14 Symposium "Fire Safety in Buildings: Needs and Criteria", held in Amsterdam 1977-06-02/03, p. 120-145.
- [2] NATIONAL SWEDISH BOARD OF PHYSICAL PLANNING AND BUILDING: Brandteknisk dimensionering (Fire Engineering Design). Comments on SBN (Swedish Building Code), No. 1976:1.
- [3] PETTERSSON, O.: Principles of Fire Engineering Design and Fire Safety of Tall Buildings. ASCE-IABSE International Conference on Planning and Design of Tall Buildings, Lehigh University, Bethlehem, Pa., August 21-26, 1972, Summary Report of Technical Committee 8, Conference Preprints, Vol. DS. - Bulletin 31, Division of Structural Mechanics and Concrete Construction, Lund Institute of Technology, Lund, 1973.
- [4] PETTERSSON, O., MAGNUSSON, S.E. and THOR, J.: Fire Engineering Design of Steel Structures. Swedish Institute of Steel Construction, Publication No. 50, Stockholm 1976 (Swedish edition 1974).
- [5] PETTERSSON, O.: Calcul Théoretique des Structures Exposées au Feu,

- Sécurité de la Construction Face à L'Incendie, Séminaire tenu à Saint-Rémy-lès Chevreuse (France) du 18 au 20 Novembre 1975, Editions Eyrolles, Paris, 1977, pp. 175-224. - Theoretical Design of Fire Exposed Structures. Bulletin 51, Division of Structural Mechanics and Concrete Construction, Lund Institute of Technology, Lund, 1976.
- [6] PETTERSSON, O. and ØDEEN, K.: Brandteknisk dimensionering av byggnadskonstruktioner - principer, underlag, exempel (Fire Engineering Design of Building Structures - Principles, Design Basis, Examples). Liber Förlag, Stockholm, 1978.
 - [7] NATIONAL SWEDISH BOARD OF PHYSICAL PLANNING AND BUILDING, Safety Group: Allmänna bestämmelser för bärande konstruktioner, AK 77, del 1. Säkerhetsbestämmelser (General Regulations for Load-Bearing Structures, AK 77, Part 1, Safety Regulations). Draft Proposal, Stockholm, 1976-11-24.
 - [8] MAGNUSSON, S.E.: Probabilistic Analysis of Fire Exposed Steel Structures. Bulletin 27, Division of Structural Mechanics and Concrete Construction, Lund Institute of Technology, Lund, 1974.
 - [9] LAW, M.: Design Guide for Fire Safety of Bare Exterior Structural Steel. 1. Theory and Validation. 2. State of the Art. Ove Arup & Partners. London, January 1977.
 - [10] BECHTOLD, R.: Zur thermischen Beanspruchung von Aussenstützen im Brandfall. Heft 37, Institut für Baustoffkunde und Stahlbetonbau, Technische Universität, Braunschweig, September 1977.
 - [11] KAWAGOE, K. and SEKINE, T.: Estimation of Fire Temperature-Time Curve in Rooms. Occasional Report No. 11, Building Research Institute, Tokyo, 1963. - KAWAGOE, K.: Estimation of Fire Temperature-Time Curve in Rooms. Research Paper No. 29, Building Research Institute, Tokyo, 1967.
 - [12] ØDEEN, K.: Theoretical Study of Fire Characteristics in Enclosed Spaces. Bulletin 19, Division of Building Construction, Royal Institute of Technology, Stockholm, 1963.

- [13] MAGNUSSON, S.E. and THELANDERSSON, S.: Temperature-Time Curves for the Complete Process of Fire Development. A Theoretical Study of Wood Fuel Fires in Enclosed Spaces. Acta Polytechnica Scandinavica, Ci 65, Stockholm, 1970.
- [14] MAGNUSSON, S.E. and THELANDERSSON, S.: A Discussion of Compartment Fires. Fire Technology, Vol. 10, No. 3, August 1974.
- [15] HARMATHY, T.Z.: A New Look at Compartment Fires. Part I, Fire Technology, Vol. 8, No. 3, August 1972, and Part II, Fire Technology, Vol. 8, No. 4, November 1972.
- [16] BABRAUSKAS, V. and WILLIAMSON, R.B.: Post-Flashover Compartment Fires. University of California, Berkeley, Fire Research Group, Report No. UCB FRG 75-1, December 1975. - Post-Flashover Compartment Fires: Basis of a Theoretical Model. Fire and Materials, Vol. 2, No. 2, April 1978.
- [17] THOMAS, P.H.: Some Problem Aspects of Fully Developed Room Fires. Symposium on "Fire Standards and Safety", Washington, 5-6 April 1976.
- [18] MAGNUSSON, S.E. and PETTERSSON, O.: Brandteknisk dimensionering av isolerad stålkonstruktion i bärande eller avskiljande funktion (Fire Engineering Design of Insulated Load-Bearing or Separating Steel Structures). Väg- och vattenbyggaren No. 4, Stockholm, 1969.
- [19] HARMATHY, T.Z.: A Treatise on Theoretical Fire Endurance Rating. Research Paper No. 153, Division of Building Research, National Research Council, Canada, Ottawa, 1962.
- [20] ÖDEEN, K. and ANÄS, B.: Brandskyddande undertak för stålkonstruktioner (Fire Protection for Steel Structures in the Form of a Suspended Ceiling). Byggmästaren No. 12, Stockholm, 1969.
- [21] WICKSTRÖM, U.: A Numerical Procedure for Calculating Temperature in Hollow Structures Exposed to Fire. Fire Research Group, University of California, Report No. UCB FRG 77-9, Berkeley, August 1977.

- [22] THOR, J.: Deformations and Critical Loads of Steel Beams Under Fire Exposure Conditions. National Swedish Building Research, Document D16:1973, Stockholm.
- [23] ROBERTSON, A.F. and RYAN, I.V.: Proposed Criteria for Defining Load Failure of Beams, Floors and Roof Constructions during Fire Tests. Journal of Research, National Bureau of Standards, Vol. 63 C, Washington, 1959.
- [24] KRUPPA, J.: Résistance au Feu des Structures Métalliques en Température Non Homogène. Thèse, Présentée devant l'Institut National des Sciences Appliquées de Rennes pour l'obtention du grade de Docteur-Ingenieur en Genie Civil, 27 Juin 1977.

Acknowledgement

This paper is mainly based on results, published in different connections, from the research activities within the fire research group at the Division of Structural Mechanics and Concrete Construction, Civil Engineering Department, Lund University. In substantial extent, this fire research is financially sponsored by the National Swedish Council for Building Research, Stockholm.

APPENDIX

Table 1. Coefficient K_f for transforming a real fire load density q and a real opening factor of a fire compartment $A\sqrt{h}/A_t$ to a fictitious fire load density q_f and a fictitious opening factor $(A\sqrt{h}/A_t)_f$ corresponding to a fire compartment, type A

$$q_f = K_f q \quad (A\sqrt{h}/A_t)_f = K_f A\sqrt{h}/A_t$$

Type of fire compartment	Opening factor $A\sqrt{h}/A_t \text{ m}^{1/2}$					
	0.02	0.04	0.06	0.08	0.10	0.12
Type A	1	1	1	1	1	1
Type B	0.85	0.85	0.85	0.85	0.85	0.85
Type C	3.00	3.00	3.00	3.00	3.00	2.50
Type D	1.35	1.35	1.35	1.50	1.55	1.65
Type E	1.65	1.50	1.35	1.50	1.75	2.00
Type F ¹⁾	1.00-	1.00-	0.80-	0.70-	0.70-	0.70-
	0.50	0.50	0.50	0.50	0.50	0.50
Type G	1.50	1.45	1.35	1.25	1.15	1.05

¹⁾ The lowest value of K_f applies to a fire load density $q > 500 \text{ MJ}\cdot\text{m}^{-2}$, the highest value to a fire load density $q \leq 60 \text{ MJ}\cdot\text{m}^{-2}$. For intermediate fire load densities, linear interpolation gives sufficient accuracy.

The different types of fire compartment are defined as follows

Fire compartment, type B: Bounding structures of concrete.

Fire compartment, type C: Bounding structures of lightweight concrete (density $\rho = 500 \text{ kg}\cdot\text{m}^{-3}$).

Fire compartment, type D: 50% of the bounding structures of concrete, and 50% lightweight concrete (density $\rho = 500 \text{ kg}\cdot\text{m}^{-3}$).

Fire compartment, type E: Bounding structures with the following percentage of bounding surface area:

50% lightweight concrete (density $\rho = 500 \text{ kg}\cdot\text{m}^{-3}$),
33% concrete,

17% of from the interior to the exterior: plasterboard panel (density $\rho = 790 \text{ kg}\cdot\text{m}^{-3}$), 13 mm in thickness - diabase wool (density $\rho = 50 \text{ kg}\cdot\text{m}^{-3}$), 10 cm in thickness - brickwork (density $\rho = 1800 \text{ kg}\cdot\text{m}^{-3}$), 20 cm in thickness.

Fire compartment, type F: 80% of the bounding structures of sheet steel, and 20% of concrete. The compartment corresponds to a storage space with a sheet steel roof, sheet steel walls, and a concrete floor.

Fire compartment, type G: Bounding structures with the following percentage of bounding surface area:

20% concrete,

80% of from the interior to the exterior: double plasterboard panel (density $\rho=790 \text{ kg}\cdot\text{m}^{-3}$), 2x13 mm in thickness - air space, 10 cm in thickness - double plasterboard panel (density $\rho = 790 \text{ kg}\cdot\text{m}^{-3}$), 2x13 mm in thickness.

For fire compartments, not directly represented in the table, the coefficient K_f can either be determined by a linear interpolation between applicable types of fire compartment in the table or be chosen in such a way as to give results on the safe side. For fire compartments with surrounding structures of both concrete and lightweight concrete, then different values can be obtained of the coefficient K_f , depending on the choice between the fire compartment types B, C, and D at the interpolation. This is due to the fact that the relationships, determining K_f , are non-linear. However, the K_f -values of the table are such that a linear interpolation always gives results on the safe side, irrespective of the alternative of interpolation chosen. In order to avoid an unnecessarily large overestimation of K_f , that alternative of interpolation is recommended which gives the lowest value of K_f .

Table 2. Maximum steel temperature $T_{s,max}$ ($^{\circ}\text{C}$) for uninsulated steel structure as a function of fictitious fire load density q ($\text{Mcal}\cdot\text{m}^{-2}$) ($\text{MJ}\cdot\text{m}^{-2}$), fictitious opening factor $A\sqrt{h}/A_t$ ($\text{m}^{1/2}$), F_s/V_s ratio (m^{-1}), and resultant emissivity ϵ_r [4]

q	AVh At	Fs Vs	Ts,max				q	AVh At	Fs Vs	Ts,max				q	AVh At	Fs Vs	Ts,max				q	AVh At	Fs Vs	Ts,max										
			er	0.3	0.5	0.7				er	0.3	0.5	0.7				er	0.3	0.5	0.7				er	0.3	0.5	0.7							
10 {42}	0,01	50	325	345	370	15 {63}	0,01	50	400	420	440	20 {84}	0,01	25	390	423	445	25 {105}	0,01	25	455	490	500	30 {126}	0,01	25	455	490	500					
		75	365	385	405			75	435	445	460			75	485	480	490			75	525	530	535			75	525	530	535					
		100	395	410	425			100	460	460	470			100	495	505	505			100	530	535	535			100	530	535	535	100	530	535	535	
		125	410	425	435			125	460	470	475			125	500	505	510			125	530	535	540			125	530	535	540	125	530	535	540	
		150	425	435	440			150	470	475	480			150	505	510	510			150	533	540	540			150	533	540	540	150	533	540	540	
		200	425	445	445			200	475	480	480			200	505	510	515			200	533	540	540			200	533	540	540	200	533	540	540	
	0,02	50	335	380	410		0,02	50	425	480	515		0,02	50	300	330	375		0,02	50	355	400	425		0,02	50	355	400	425	0,02	50	355	400	425
		75	410	445	475			75	500	540	565			75	560	600	620			75	610	640	650			75	610	640	650		75	610	640	650
		100	445	490	520			100	540	575	595			100	595	620	630			100	640	650	655			100	640	650	655		100	640	650	655
		125	480	520	545			125	565	600	610			125	615	630	640			125	650	655	660			125	650	655	660		125	650	655	660
		150	500	540	555			150	585	605	615			150	625	640	645			150	670	675	680			150	670	675	680		150	670	675	680
		200	540	560	575			200	605	620	625			200	635	645	650			200	675	680	685			200	675	680	685		200	675	680	685
	0,04	50	285	320	365		0,04	50	400	455	510		0,04	50	495	565	625		0,04	50	495	565	625		0,04	50	495	565	625	0,04	50	495	565	625
		75	350	400	450			75	490	530	600			75	560	630	700			75	560	630	700			75	560	630	700		75	560	630	700
		100	405	460	510			100	550	610	655			100	630	700	740			100	630	700	740			100	630	700	740		100	630	700	740
		125	450	515	535			125	600	655	690			125	685	735	755			125	685	735	755			125	685	735	755		125	685	735	755
		150	495	555	595			150	635	680	710			150	725	775	795			150	725	775	795			150	725	775	795		150	725	775	795
		200	530	605	645			200	650	700	735			200	745	795	815			200	745	795	815			200	745	795	815		200	745	795	815
	0,06	50	235	275	330		0,06	50	340	400	475		0,06	50	390	460	530		0,06	50	390	460	530		0,06	50	390	460	530	0,06	50	390	460	530
		75	305	370	425			75	425	490	575			75	495	565	635			75	495	565	635			75	495	565	635		75	495	565	635
		100	365	410	455			100	500	550	630			100	575	630	700			100	575	630	700			100	575	630	700		100	575	630	700
		125	415	450	545			125	550	600	680			125	625	680	735			125	625	680	735			125	625	680	735		125	625	680	735
		150	450	485	580			150	590	630	720			150	665	715	770			150	665	715	770			150	665	715	770		150	665	715	770
		200	520	550	660			200	650	700	755			200	735	785	815			200	735	785	815			200	735	785	815		200	735	785	815
0,08	50	200	250	300	0,08	50	300	375	430	0,08	50	330	400	460	0,08	50	330	400	460	0,08	50	330	400	460	0,08	50	330	400	460					
	75	270	330	400		75	380	465	535		75	410	495	565		75	410	495	565		75	410	495	565		75	410	495	565					
	100	330	400	460		100	450	545	605		100	485	570	635		100	485	570	635		100	485	570	635		100	485	570	635					
	125	360	450	510		125	500	595	670		125	535	630	700		125	535	630	700		125	535	630	700		125	535	630	700					
	150	410	510	560		150	555	650	710		150	590	685	745		150	590	685	745		150	590	685	745		150	590	685	745					
	200	480	590	660		200	625	725	785		200	660	760	815		200	660	760	815		200	660	760	815		200	660	760	815					
0,12	50	170	200	255	0,12	50	260	290	400	0,12	50	260	290	400	0,12	50	260	290	400	0,12	50	260	290	400	0,12	50	260	290	400					
	75	220	260	350		75	340	380	500		75	340	380	500		75	340	380	500		75	340	380	500		75	340	380	500					
	100	240	310	400		100	360	430	530		100	360	430	530		100	360	430	530		100	360	430	530		100	360	430	530					
	125	260	380	540		125	400	450	605		125	400	450	605		125	400	450	605		125	400	450	605		125	400	450	605					
	150	310	430	620		150	460	475	635		150	460	475	635		150	460	475	635		150	460	475	635		150	460	475	635					
	200	380	500	700		200	500	500	665		200	500	500	665		200	500	500	665		200	500	500	665		200	500	500	665					
12,5 {52,5}	0,01	50	365	385	405	17,5 {73,5}	0,01	50	460	515	550	22,5 {94,5}	0,01	25	430	460	480	25 {105}	0,01	25	495	530	550	30 {126}	0,01	25	495	530	550					
		75	415	485	540			75	530	570	595			50	495	565	625			50	565	600	610			50	565	600	610					
		100	430	445	450			100	565	600	615			75	620	690	730			75	690	730	740			75	690	730	740					
		125	440	450	460			125	595	610	630			100	680	740	760			100	740	760	770			100	740	760	770					
		150	450	455	460			150	610	620	635			125	700	750	770			125	750	770	780			125	750	770	780					
		200	455	460	465			200	625	635	645			150	735	785	805			150	785	805	815			150	785	805	815					
	0,02	50	380	435	470		0,02	50	480	535	570		0,02	50	430	460	480		0,02	50	495	530	550		0,02	50	495	530	550					
		75	455	500	535			75	545	600	655			75	580	650	710			75	580	650	710			75	580	650	710					
		100	500	540	560			100	600	660	705			100	660	720	760			100	660	720	760			100	660	720	760					
		125	550	570	580			125	635	645	645			125	665	725	735			125	665	725	735			125	665	725	735					
		150	550	570	580			150	635	645	645			150	665	725	735			150	665	725	735			150	665	725	735					
		200	570	590	600			200	650	660	660			200	670	730	780			200	670	730	780			200	670	730	780					
0,04	50	340	400	450	0,04	50	450	515	575	0,04	50	430	460	480	0,04	50	495	530	550	0,04	50	495	530	550										
	75	415	485	540		75	545	600	655		75	580	650	710		75	580	650	710		75	580	650	710										
	100	485	530	600		100	600	660	705		100	660	720	760		100	660	720	760		100	660	720	760										
	125	570	620	645		125	635	645	645		125	665	725	735		125	665	725	735		125	665	725	735										
	150	570	620	645		150	635	645	645		150	665	725	735		150	665	725	735		150	665	725	735										
	200	630	665	700		200	650	660	660		200	670	730	780		200	670	730	780		200	670	730	780										
0,06	50	290	335	400	0,06	50	390	455	530	0,06	50	390	460	530	0,06	50	390	460	530	0,06	50	390	460	530										
	75	365	425	495		75	490	555	635		75	490	555	635		75	490	555	635		75	490	555	635										
	100	425	480	560		100	565	620	710		100	565	620	710		100	565	620	710		100	565	620	710										
	125	480	525	610		125	600	650	740		125	600	650	740		125	600	650	740		125	600	650	740										
	150	520	560	650		150	625	670	750		150	625	670	750		150	625	670	750		150	625	670	750										
	200	580	625	705		200	650	660	660		200	670	730	780		200	670	730	780		200	670	730	780										
0,08	50	250	315	360	0,08	50	345	435	490	0,08	50	390	460	530	0,08	50	390	460	530	0,08	50	390	460	530										
	75	325	400	455		75	440	530	600		75	440	530	600		75	440	530	600		75	440	530	600										

Table 3. Maximum steel temperature $T_{s,max}$ ($^{\circ}\text{C}$) for insulated steel structure as a function of fictitious fire load density q ($\text{Mcal}\cdot\text{m}^{-2}$) [$\text{MJ}\cdot\text{m}^{-2}$], fictitious opening factor AV_h/A_t ($\text{m}^{1/2}$), structural parameter A_i/V_s (m^{-1}), and insulation parameter d_i/λ_i ($\text{m}^2\cdot^{\circ}\text{C}\cdot\text{h}\cdot\text{kcal}^{-1}$)^a. d_i denotes insulation thickness (m) [4]

	$\frac{AV_h}{A_t}$	$\frac{A_i}{V_s}$	$T_{s,max}$					q	$\frac{AV_h}{A_t}$	$\frac{A_i}{V_s}$	$T_{s,max}$					q	$\frac{AV_h}{A_t}$	$\frac{A_i}{V_s}$	$T_{s,max}$					q	$\frac{AV_h}{A_t}$	$\frac{A_i}{V_s}$	$T_{s,max}$									
			d_i/λ_i	d_i/λ_i	d_i/λ_i	d_i/λ_i					d_i/λ_i	d_i/λ_i	d_i/λ_i	d_i/λ_i	d_i/λ_i				d_i/λ_i	d_i/λ_i	d_i/λ_i	d_i/λ_i	d_i/λ_i				d_i/λ_i	d_i/λ_i	d_i/λ_i	d_i/λ_i	d_i/λ_i	d_i/λ_i	d_i/λ_i	d_i/λ_i	d_i/λ_i	
15 {63}	0,01	100	380	325	255	215		0,01	50	430	360	275	230		0,02	25	360	260	185	145		0,02	25	445	330	230	180									
		125	405	350	280	240			75	470	410	330	275			50	490	380	270	225			50	570	460	340	275									
		150	420	365	300	260			100	495	445	370	320			75	550	445	340	280			75	640	540	415	340									
		200	440	395	335	290			125	505	465	395	350			100	595	490	385	325			100	670	580	470	395									
		300	460	430	375	335			150	515	480	420	375			125	625	535	425	360			125	695	620	510	440									
	400	470	445	405	370		200		525	500	450	410		200		645	555	460	395		150		710	650	550	475										
	0,02	100	390	300	220	180		0,02	400	535	530	505	480			0,04	100	665	600	510	445			0,04	100	725	680	600	530							
		125	420	340	250	205			50	395	300	225	180				300	690	640	580	515				300	740	710	655	600							
		150	450	360	275	225			75	455	360	290	230				400	700	670	610	560				400	745	730	680	640							
		200	500	400	310	260			100	500	405	310	260				25	275	200	130	100				25	330	245	160	125							
300		550	460	370	320		125	540	445	350	300		50	410	300		205	160		50	480	360	250		195											
400	575	505	415	355		150	560	470	375	320		75	500	380	265	210		75	565	440	315	250														
20 {64}	0,01	100	375	270	195	155		0,01	50	400	295	200	160		0,04	100	560	440	310	250		0,04	100	630	500	370	300									
		125	400	300	210	175			75	430	330	240	195			125	610	480	350	280			125	680	550	410	340									
		150	430	350	250	205			100	450	350	260	210			150	650	525	385	310			150	715	590	450	370									
		200	450	370	280	210			125	480	380	290	235			200	700	590	445	370			200	765	650	510	430									
		300	470	390	300	240			150	500	400	310	260			300	760	665	530	450			300	-	725	600	510									
	400	490	410	320	260		200		520	420	330	280		400		-	710	585	510		400		-	770	655	580										
	0,02	100	350	255	185	145		0,02	75	350	245	170	130			0,06	100	595	455	320	260			0,06	100	660	520	380	305							
		125	380	285	200	160			100	350	245	170	130				150	595	455	320	260				150	665	530	390	310							
		150	400	300	210	175			125	400	290	195	155				200	660	520	380	305				200	750	610	465	380							
		200	430	350	250	205			150	455	330	230	185				300	750	610	465	380				300	800	675	530	440							
300		450	370	280	210		200	480	380	290	235		400	800	675		530	440		400	800	675	530		440											
400	470	390	300	240		300	500	400	310	260		50	350	250	165	125		50	420	300	200	155														
25 {65}	0,01	100	350	250	175	140		0,01	50	330	235	165	125		0,06	100	555	415	295	235		0,06	100	595	455	320	260									
		125	380	285	200	160			75	350	245	170	130			150	595	455	320	260			150	665	530	390	310									
		150	400	300	210	175			100	350	245	170	130			200	660	520	380	305			200	750	610	465	380									
		200	430	350	250	205			125	400	290	195	155			300	750	610	465	380			300	800	675	530	440									
		300	450	370	280	210			150	455	330	230	185			400	800	675	530	440			400	800	675	530	440									
	400	470	390	300	240		200		480	380	290	235		50		330	235	165	125		50		420	300	200	155										
	0,02	100	330	250	175	140		0,02	75	330	235	165	125			0,08	100	540	405	290	225			0,08	100	580	440	310	250							
		125	360	270	195	155			100	330	235	165	125				150	540	405	290	225				150	610	470	340	265							
		150	390	290	200	160			125	360	270	195	155				200	610	470	340	265				200	715	570	430	345							
		200	420	320	230	185			150	390	290	200	160				300	715	570	430	345				300	-	640	490	400							
300		440	340	250	195		200	420	320	230	185		400	-	640		490	400		400	-	640	490		400											
400	460	360	270	210		300	450	350	260	210		50	375	265	170	135		50	450	325	225	175														
30 {66}	0,01	100	330	250	175	140		0,01	50	310	215	155	115		0,12	100	465	325	225	180		0,12	100	500	355	250	195									
		125	360	270	195	155			75	310	215	155	115			150	465	325	225	180			150	530	400	280	220									
		150	390	290	200	160			100	310	215	155	115			200	500	355	250	195			200	580	450	310	250									
		200	420	320	230	185			125	340	240	160	120			300	580	450	310	250			300	675	505	370	300									
		300	440	340	250	195			150	370	270	185	140			400	675	505	370	300			400	760	600	470	380									
	400	460	360	270	210		200		400	300	210	165		50		330	235	165	125		50		425	300	205	160										
	0,02	100	310	215	155	115		0,02	75	310	215	155	115			0,04	100	445	305	205	160			0,04	100	480	340	240	180							
		125	340	240	160	120			100	310	215	155	115				150	445	305	205	160				150	500	355	250	195							
		150	370	270	185	140			125	340	240	160	120				200	480	340	240	180				200	560	415	335								
		200	400	300	210	165			150	370	270	185	140				300	560	415	335			300		640	490	350	285								
300		420	320	230	185		200	400	300	210	165		400	640	490		350	285		400	720	570	430		350											
400	440	340	250	195		300	430	330	240	185		50	350	250	165	125		50	440	320	220	175														
35 {67}	0,01	100	310	215	155	115		0,01	50	290	195	140	100		0,12	100	425	285	185	145		0,12	100	460	320	220	180									
		125	340	240	160	120			75	290	195	140	100			150	425	285	185	145			150	490	340	240	180									
		150	370	270	185	140			100	290	195	140	100			200	460	320	220	180			200	540	390	290	230									
		200	400	300	210	165			125	320	220	160	120			300	540	390	290	230			300	620	470	370	310									
		300	420	320	230	185			150	350	250	165	125			400	620	470	370	310			400	700	550	450	390									
	400	440	340	250	195		200		380	280	190	140		50		330	235	165	125		50		420	300	205	160										
	0,02	100	290	195	140	100		0,02	75	290	195	140	100			0,06	100	405	265	165	125			0,06	100	440	285	185	145							
		125	320	220	160	120			100	290	195	140	100				150	405	265	165	125				150	475	325	225	185							
		150	350	250	165	125			125	320	220	160	120				200	440	285	185	145				200	510	360	260	200							
		200	380	280	190	140			150	350	250	165	125				300	510	360	260	200				300	590	440	340	280							
300		400	300	210	165		200	380	280	190	140		400	590	440		340	280		400	670	520	420		360											
400	420	320	230	185		300	410	310	220	170		50	340	240	155	120		50	430	310	210	165														
40 {68}	0,01	100	290	195	140	100		0,01	50	270	175	130	90		0,12	100	400	260	160	120		0,12	100	435	275	175	135									
		125	320	220	160	120			75	270	175	130	90			150	400	260	160	120			150	470	310	210	165									
		150	350	250</																																

q	$\frac{AV\sqrt{h}}{A_t}$	$\frac{A_i}{V_s}$	$T_{s,max}$					q	$\frac{AV\sqrt{h}}{A_t}$	$\frac{A_i}{V_s}$	$T_{s,max}$					q	$\frac{AV\sqrt{h}}{A_t}$	$\frac{A_i}{V_s}$	$T_{s,max}$					
			d_{ij}/λ_i	d_{ij}/λ_j	d_{ij}/λ_i	d_{ij}/λ_j	d_{ij}/λ_i				d_{ij}/λ_j	d_{ij}/λ_i	d_{ij}/λ_j	d_{ij}/λ_i	d_{ij}/λ_j									
																			0,05	0,10	0,20	0,30	0,05	0,10
50 [210]	0,02	25	480	355	250	200	0,02	25	550	420	295	235	0,04	25	325	395	270	205	0,04	25	660	500	350	270
		50	605	490	375	300		50	665	560	430	350		50	665	540	400	320		50	-	670	520	420
		75	665	570	450	380		75	715	640	515	435		75	735	625	490	400		75	-	760	620	520
		100	700	620	510	435		100	745	675	570	495		100	790	680	550	435		100	-	-	695	595
		125	720	650	550	475		125	760	705	610	540		125	-	710	600	505		125	-	-	745	650
		150	730	675	585	510		150	770	725	640	575		150	-	750	640	550		150	-	-	-	-
	0,04	200	745	700	630	565	200	780	750	690	625	200	-	800	695	605	200	-	-	-	-			
		300	755	735	680	635	300	-	-	-	-	300	-	-	-	-	300	-	-	-	-			
		25	350	255	170	135	0,04	25	405	300	200	150	0,06	25	400	280	185	140	0,06	25	565	415	285	225
		50	500	385	270	210		50	560	430	305	240		50	565	415	285	225		50	-	675	500	405
		75	600	460	340	265		75	650	515	380	310		75	670	510	365	290		75	-	750	575	475
		100	655	525	395	315		100	715	580	440	360		100	740	585	425	345		100	-	-	635	535
125	705	575	435	355	125	755		640	490	405	125	790		640	480	390	125	-		-	685	585		
150	740	615	475	395	150	790		675	530	440	150	-		685	525	430	150	-		-	-	-		
0,06	200	785	675	540	450	200	-	730	600	505	300	-	755	650	500	200	-	-	-	-				
	300	-	750	625	545	300	-	795	680	590	400	-	-	695	600	300	-	-	-	-				
	25	300	210	135	105	0,06	25	345	240	155	120	0,08	25	350	240	160	120	0,08	25	475	325	220	165	
	50	445	320	215	170		50	500	380	240	195		50	510	385	250	190		50	560	490	340	260	
	75	540	400	275	220		75	600	450	315	250		75	615	455	320	250		75	770	595	435	340	
	100	610	465	330	260		100	670	515	375	300		100	700	530	375	300		100	-	-	670	505	400
125	665	515	375	300	125		725	570	415	340	125		750	585	425	340	125		-	-	740	560	450	
150	710	560	410	330	150		765	615	460	375	150		800	640	470	385	150		-	-	780	610	500	
0,08	200	775	625	475	395	200	-	685	525	435	300	-	710	545	450	200	-	-	-	-				
	300	-	725	570	480	300	-	775	625	530	400	-	-	650	550	300	-	-	-	-				
	400	-	700	635	545	400	-	-	695	600	400	-	-	730	625	400	-	-	-	-				
	25	300	200	135	100	0,08	25	300	200	135	100	0,12	25	420	290	190	150	0,12	25	390	250	165	130	
	50	450	315	210	160		50	450	315	210	160		50	525	375	250	200		50	565	390	260	210	
	75	550	400	275	210		75	615	460	325	255		75	600	440	300	240		75	690	495	340	270	
100	615	460	325	255	100		680	515	365	290	100		680	500	350	275	100		750	565	400	320		
125	680	515	365	290	125		725	560	400	330	125		725	550	390	300	125		-	-	640	450	370	
150	725	560	400	330	150		765	615	460	375	150		800	620	450	360	150		-	-	690	500	410	
0,10	200	800	640	475	390	200	-	750	580	480	300	-	730	550	450	200	-	-	-	-				
	300	-	750	580	480	300	-	-	650	550	400	-	-	800	650	520	300	-	-	-	-			
	400	-	-	-	-	400	-	-	-	-	400	-	-	-	-	400	-	-	-	-				
	50	370	250	160	125	0,12	50	370	250	160	125	0,30	50	305	205	135	105	0,30	50	435	300	195	150	
	75	470	330	210	170		75	470	330	210	170		75	410	285	190	150		75	435	300	195	150	
	100	550	385	250	200		100	550	385	250	200		100	465	315	210	170		100	510	355	235	180	
125	600	430	300	235	125		600	430	300	235	125		535	365	255	200	125		375	410	270	210		
150	650	480	330	265	150		650	480	330	265	150		635	480	335	260	150		625	455	305	240		
200	735	550	400	310	200		735	550	400	310	200		715	530	390	310	200		705	530	365	295		
0,12	300	-	660	500	400	300	-	750	575	465	400	-	-	-	-	300	-	-	-	-				
	400	-	-	-	-	400	-	-	-	-	400	-	-	-	-	400	-	-	-	-				
	25	345	235	155	125	0,12	25	395	265	175	145	0,04	25	450	315	210	160	0,04	25	450	315	210	160	
	50	460	325	215	165		50	460	325	215	165		50	470	320	220	175		50	475	320	220	175	
	75	535	365	245	195		75	535	365	245	195		75	580	415	285	225		75	580	415	285	225	
	100	600	430	300	235		100	600	430	300	235		100	670	495	340	275		100	670	495	340	275	
125	650	480	330	265	125		650	480	330	265	125		740	550	395	305	125		740	550	395	305		
150	700	530	375	295	150		700	530	375	295	150		800	600	440	350	150		800	600	440	350		
0,14	200	-	680	500	405	200	-	775	600	500	300	-	-	-	-	200	-	-	-	-				
	300	-	780	600	440	300	-	800	605	505	400	-	-	-	-	300	-	-	-	-				
	400	-	-	-	-	400	-	-	-	-	400	-	-	-	-	400	-	-	-	-				
	25	320	210	140	105	0,14	25	320	210	140	105	0,08	25	400	275	180	140	0,08	25	400	275	180	140	
	50	475	330	220	175		50	475	330	220	175		50	570	415	285	220		50	570	415	285	220	
	75	590	425	285	225		75	590	425	285	225		75	680	510	360	285		75	680	510	360	285	
100	670	495	340	275	100		670	495	340	275	100		755	590	420	340	100		755	590	420	340		
125	740	550	395	305	125		740	550	395	305	125		-	650	480	390	125		-	-	700	520	430	
150	800	600	440	350	150		800	600	440	350	150		-	700	520	430	150		-	-	700	520	430	
0,16	200	-	680	500	405	200	-	775	600	500	300	-	-	-	-	200	-	-	-	-				
	300	-	780	600	440	300	-	800	605	505	400	-	-	-	-	300	-	-	-	-				
	400	-	-	-	-	400	-	-	-	-	400	-	-	-	-	400	-	-	-	-				
	25	320	210	140	105	0,16	25	320	210	140	105	0,12	25	400	275	180	140	0,12	25	400	275	180	140	
	50	475	330	220	175		50	475	330	220	175		50	570	415	285	220		50	570	415	285	220	
	75	590	425	285	225		75	590	425	285	225		75	680	510	360	285		75	680	510	360	285	
100	670	495	340	275	100		670	495	340	275	100		755	590	420	340	100		755	590	420	340		
125	740	550	395	305	125		740	550	395	305	125		-	650	480	390	125		-	-	700	520	430	
150	800	600	440	350	150		800	600	440	350	150		-	700	520	430	150		-	-	700	520	430	
0,18	200	-	680	500	405	200	-	775	600	500	300	-	-	-	-	200	-	-	-	-				
	300	-	780	600	440	300	-	800	605	505	400	-	-	-	-	300	-	-	-	-				
	400	-	-	-	-	400	-	-	-	-	400	-	-	-	-	400	-	-	-	-				
	25	320	210	140	105	0,18	25	320	210	140	105	0,30	25	450	315	210	160	0,30	25	450	315	210	160	
	50	475	330	220	175		50	475	330	220	175		50	570	415	285	220		50	570	415	285	220	
	75	590	425	285	225		75	590	425	285	225		75	680	510	360	285		75	680	510	360	285	
100	670	495	340	275	100		670	495	340	275	100		755	590	420	340	100		755	590	420	340		
125	740	550	395	305	125		740	550	395	305	125		-	650	480	390	125		-	-	700	520	430	
150	800	600	440	350	150		800	600	440	350	150		-	700	520	430								

Table 4. Maximum steel temperature $T_{s,max}$ ($^{\circ}\text{C}$) for a steel structure insulated with gypsum plaster slabs, type Gyproc ($\rho_i = 790 \text{ kg}\cdot\text{m}^{-3}$), as a function of fictitious fire load density q ($\text{Mcal}\cdot\text{m}^{-2}$) ($\text{MJ}\cdot\text{m}^{-2}$), fictitious opening factor $A\sqrt{h}/A_t$ ($\text{m}^{1/2}$), structural parameter A_i/V_s (m^{-1}), and insulation thickness d_i (mm) [4]

q	$A\sqrt{h}/A_t$	A_i/V_s	$T_{s,max}$		q	$A\sqrt{h}/A_t$	A_i/V_s	$T_{s,max}$		q	$A\sqrt{h}/A_t$	A_i/V_s	$T_{s,max}$		q	$A\sqrt{h}/A_t$	A_i/V_s	$T_{s,max}$	
			d_i	d_i				d_i	d_i				d_i	d_i				d_i	d_i
			13	26				13	26				13	26				13	26
15 [63]	0,01	125	315	200	30 [126]	0,01	25	315	210	40 [108]	0,02	25	305	195	50 [210]	0,02	25	390	250
			150	335				50	415				50	435				50	550
			200	365				75	465				75	525				75	635
			300	395				100	495				100	600				100	725
	0,02	125	300	150		0,02	125	510	420		0,02	125	640	425		0,04	125	755	615
			150	325				150	525				150	675				150	765
			200	350				200	535				200	700				200	800
			300	405				300	550				300	720				300	850
	0,04	125	400	230		0,04	125	560	510		0,04	125	650	500		0,04	125	745	680
			300	300				50	350				50	425				50	510
			400	330				75	410				75	485				75	580
			400	330				100	460				100	535				100	630
20 [84]	0,01	75	345	230	30 [126]	0,02	150	320	365	40 [108]	0,02	150	420	215	50 [210]	0,06	150	600	375
			100	380				200	370				200	450				200	550
			125	405				300	440				300	520				300	630
			200	440				400	480				400	560				400	675
	0,02	75	300	180		0,04	150	470	260		0,06	150	600	300		0,08	150	750	535
			100	345				125	435				125	485				125	580
			125	375				200	520				200	600				200	700
			150	400				300	630				300	730				300	850
	0,04	75	300	180		0,06	150	395	175		0,08	150	445	220		0,12	150	650	375
			100	325				125	365				125	400				125	475
			125	375				200	445				200	520				200	630
			150	400				300	550				300	650				300	775
25 [105]	0,01	50	360	250	35 [147]	0,02	50	390	255	45 [190]	0,02	50	495	335	60 [250]	0,02	50	690	430
			75	410				75	465				75	600				75	770
			100	440				100	520				100	685				100	850
			125	470				125	560				125	715				125	880
	0,02	50	300	175		0,04	50	310	170		0,04	50	380	230		0,06	50	470	390
			75	355				75	385				75	460				75	575
			100	400				100	445				100	525				100	630
			125	430				125	490				125	585				125	695
	0,04	50	300	175		0,06	50	310	170		0,08	50	340	200		0,12	50	400	295
			75	355				75	385				75	460				75	575
			100	400				100	445				100	525				100	630
			125	430				125	490				125	585				125	695

Table 5. Maximum steel beam temperature $T_{s,max}$ ($^{\circ}\text{C}$) for a steel beam construction according to Fig. 10, with an insulation in the form of a suspended ceiling, as a function of fictitious fire load density q ($\text{Mcal}\cdot\text{m}^{-2}$) ($\text{MJ}\cdot\text{m}^{-2}$), fictitious opening factor $A\sqrt{h}/A_t$ ($\text{m}^{1/2}$), structural parameter F_s/V_s (m^{-1}), and insulation parameter d_i/λ_i ($\text{m}^2\cdot^{\circ}\text{C}\cdot\text{h}\cdot\text{kcal}^{-1}$)^c. The maximum temperature in the suspended ceiling is given in brackets [4]

q	$\frac{A\sqrt{h}}{A_t}$	$\frac{F_s}{V_s}$	Maximum steel temperature $T_{s,max}$ and () maximum suspended ceiling temperature				q	$\frac{A\sqrt{h}}{A_t}$	$\frac{F_s}{V_s}$	Maximum steel temperature $T_{s,max}$ and () maximum suspended ceiling temperature			
			$(d_i/\lambda_i)_{fict}$							$(d_i/\lambda_i)_{fict}$			
			0,05	0,10	0,20	0,30				0,05	0,10	0,20	0,30
15 {63}	0,02	50	130	90	65	50	60 {250}	0,02	50	435	315	200	160
		100	180	130	90	70			100	450	340	240	185
		200	230 (470)	170 (440)	115 (410)	90 (390)			200	455 (615)	350 (570)	250 (530)	200 (500)
		300	260	190	130	100			300	455	350	250	200
	0,04	50	100	70	45	40		0,04	50	340	225	145	110
		100	150 (565)	100 (530)	65 (500)	50 (475)			100	400 (680)	285 (630)	185 (590)	140 (560)
		200	200	140	90	70 (475)			200	435 (680)	320 (630)	220 (590)	165 (560)
		300	240	170	110	80			300	445	330	230	180
	0,08	50	65	50	35	25		0,08	50	250	160	100	75
		100	95	70	50	40			100	340	225	130	100
		200	150 (675)	100 (630)	65 (590)	50 (570)			200	415 (750)	285 (700)	185 (630)	135 (625)
		300	190	125	90	60			300	445	315	210	155
0,12	50	40	35	30	25	0,12	50	190	120	75	60		
	100	60	45	40	30 (620)		100	285 (780)	185 (725)	110 (680)	80 (660)		
	200	120 (735)	70	50	40		200	375	250	155	110		
	300	155	100	60	45		300	420	290	185	130		
25 {105}	0,02	50	200	140	95	75	90 {380}	0,04	50	475	330	205	150
		100	260	185	125	100 (420)			100	510 (740)	370 (680)	250 (630)	190 (600)
		200	300 (510)	225 (470)	155 (435)	120			200	515 (740)	385 (680)	270 (630)	210 (600)
		300	320	245	170	130			300	515	385	270	215
	0,04	50	160	110	75	55		0,08	50	345	225	130	100
		100	230 (600)	150 (565)	100 (530)	75 (515)			100	430 (790)	290 (730)	180 (675)	130 (630)
		200	290	205 (565)	135 (530)	100 (515)			200	480	340	225 (675)	170 (630)
		300	325	235	155	115			300	495	360	250	190
	0,08	50	115	75	50	40		0,12	50	560	400	260	200
		100	160 (680)	110 (635)	70 (595)	55 (570)			100	570 (780)	420 (715)	290 (660)	220 (630)
		200	240	160	100	75			200	575	425	300	230
		300	285	195	120	90			300	575	425	300	230
40 {168}	0,02	50	80	60	40	30	120 {500}	0,04	50	425	280	160	120
		100	130	80	60	45			100	495	345	210	160
		200	190 (740)	125 (690)	80 (650)	60 (620)			200	520 (810)	375 (750)	250 (695)	195 (670)
		300	235	160	100	75			300	525	385	260	205
	0,04	50	300	220	145	110		0,08	50	240	160	105	80
		100	360 (560)	260 (520)	175 (480)	135 (460)			100	315 (645)	220 (600)	140 (560)	100 (535)
		200	380	290	200	160			200	375	270	180	135
		300	385	295	210	165			300	390	290	195	150
	0,12	50	170	110	70	55		0,12	50	130	85	55	45
		100	245 (715)	160 (665)	100 (625)	75 (600)			100	200	130	85	60
		200	335	220	140	105			200	290 (750)	190 (700)	115 (660)	85 (630)
		300	380	260	165	120			300	340	225	145	100

$C \begin{cases} 0,05 \text{ m}^2 \text{ } ^\circ\text{C/h/kcal} & = 0,043 \text{ m}^2 \text{ } ^\circ\text{C/W} \\ 0,10 & \text{ } & = 0,086 & \text{ } \\ 0,20 & \text{ } & = 0,172 & \text{ } \\ 0,30 & \text{ } & = 0,258 & \text{ } \end{cases}$

$$^c \begin{cases} 0,05 \text{ m}^2 \cdot ^{\circ}\text{C}\cdot\text{h}/\text{kcal} = 0,043 \text{ m}^2 \cdot ^{\circ}\text{C}/\text{W} \\ 0,10 \text{ } > > > = 0,086 \text{ } > > > \\ 0,20 \text{ } > > > = 0,172 \text{ } > > > \\ 0,30 \text{ } > > > = 0,258 \text{ } > > > \end{cases}$$

Table 6. Summary results of standard fire resistance tests on some types of suspended ceilings and connected values, derived from the test results, for $(d_i/\lambda_i)_{fict}$ and critical temperature of the ceilings [4]

No	Make	Material	Resistance time in standard fire test (min)	Remarks	Estimated $(d_i/\lambda_i)_{fict}$		Estimated critical suspended ceiling temperature (°C)
					$\left(\frac{m^2 \cdot ^\circ C h}{kcal}\right)$	$\left(\frac{m^2 \cdot ^\circ C}{W}\right)$	
1	Gyproc	2x13 mm gypsum plaster slabs no glass fibre reinforcement	30-40	All tests were discontinued because the suspended ceiling fell down. The critical temperature had not been reached in the steel girders	0,075	0,064	625
2		1x13 mm gypsum plaster slabs 0.25% g f r	48		0,075	0,064	650
3		1x16 mm gypsum plaster slabs 0.25% g f r	49		0,10	0,086	650
4		2x13 mm gypsum plaster slabs 0.25% g f r	60		0,15	0,129	650
5		3x13mm gypsum plaster slabs 0.25% g f r	75-80		0,25	0,215	625
6		2x20 mm gypsum plaster slabs 0.25% g f r	80		0,30	0,258	625
7	WST	2x13 mm gypsum plaster slabs with 13 mm mineral wool between them	45	All tests were discontinued for the same reason as above. The gypsum plaster slabs were not reinforced	0,30	0,258	550
8		2x13 mm gypsum plaster slabs with 13 mm mineral wool between them	50		0,30	0,258	550
9		2x13 mm gypsum plaster slabs with 43 mm straw between them	47		0,30	0,258	550
10		2x13mm gypsum plaster slabs with 43 mm straw between them	54		0,30	0,258	550
11	Ingenjör-firma Zero	Soundex special suspended ceiling tiles. Cast glass fibre reinforced gypsum plaster tiles with "ridges" in a grid pattern. Tile thickness 18 mm, at the ridges 38 mm	90	Parts of the ceiling fell down after 90 minutes. Max. steel temperature approx. 440°C	0,15	0,129	700
12	Consensus	Armstrong 13 mm thick	30	No visible damage to suspended ceiling. Max steel temperature about 450 °C	0,05	0,043	550
13		Mineral wool acoustic 16 mm thick	80		0,075	0,064	>(725) ^a
14		Type minaboard 13 mm thick	85	No visible damage to suspended ceiling. Max steel temperature about 300 °C	0,075	0,064	>(725) ^a
15	Dansk Eternitfabrik	Deflamit-Asbestolux 9 mm Deflamit + 15 mm mineral wool + 8 mm eternit	90		0,20	0,172	>(679) ^a
16	Nordakustik	Celotex Acoustiformat 15 mm thick glass fibre slab	90		0,10	0,086	(725) ^a
17	Rockwool	Rockfon Decor 85l (15 mm thick mineral wool slab)	60	No visible damage to suspended ceiling. Max steel temperature about 450 °C. The test was discontinued because the suspended ceiling fell down. The critical temperature had not been reached in the steel girders.	0,20	0,172	600

^a No damage to the suspended ceiling. Calculated temperature in the suspended ceiling when the test was discontinued.